國立臺灣大學環境工程學研究所
碩士論文
Graduate Institute of Environmental Engineering
College of Engineering
National Taiwan University
Master Thesis

以高錳酸鹽活化溶解態全氟辛酸在超聲波系統中的分解與脫氟之研究

Decomposition and Defluorination of Dissolved Perfluorooctanoic Acid in Permanganate-activated Ultrasonic System

胡奕博
Yi-Bo Hu

指導教授：駱尚廉 教授
Advisor: Professor Shang-Lien Lo

中華民國 102 年 6 月
June, 2013

國立臺灣大學碩士學位論文
口試委員會審定書

以高錳酸鹽活化溶解態全氟辛酸
在超聲波系統中的分解與脫氟之研究

Decomposition and Defluorination
of Dissolved Perfluorooctanoic Acid
in Permanganate-activated Ultrasonic System

本論文係胡奕博君（學號 R00541136）在國立臺灣大學環境工程學研究所完成之碩士學位論文，於民國 102 年 6 月 6 日承下列考試委員審查通過及口試及格，特此證明

論文審查委員：

駱尚廉

駱尚廉 博士
國立台灣大學環境工程學研究所特聘教授

林正芳

林正芳 博士
國立台灣大學環境工程學研究所教授

胡景堯

胡景堯 博士
台北醫學大學公共衛生學系助理教授

指導教授：駱尚廉

所　　長：張能復

誌謝

本碩士論文的順利完成，首先特別感謝我敬愛的指導教授駱尚廉老師，不僅讓我在來臺之初成為駱家班的一員，并在接下來的兩年時間裡，耐心地在學習、研究與生活上給予我指導與幫助。在駱教授的悉心教導下，我獲得一次學年獎學金與兩次論文競賽獎。駱教授嚴謹的時間觀念與治學態度更是我們學習的典範。同時也要感謝論文口試委員林正芳教授與胡景堯教授在百忙中對研究內容的指正與建議，使本論文趨於完善，僅此至上誠摯的謝意。

還要特別感謝李育輯博士與林怡欣學姐在研究起航之初,對我的引導與扶持,使我快速地進入研究軌道；感謝陳孟加學長不辭辛苦地在整個實驗過程中對我的指導與幫助,確保了研究的順利進行。在台灣研習碩士期間,也要感謝蔡皓程博士、黃君傑學長與葉致榮學長耐心、慷慨地與我討論研究方向、實驗設計與論文技巧，無疑提升了本研究的容量與深度。

在研究所的學習與生活中，要感謝 GIEE 100 級全體同學的陪伴與協助，感謝楷堯、安琪、曉玫、怡君、又楚、凱仁、智開、欣叡、智揚、瑋仁、勁妤、重愷、枋霖、炯文、光傑、博傑、海翔、聲富、哲賢、冠霖、政達、峻賢、冠沂、峻豪、劭宇、書弘、雅婷、皓瑜、嘉璘、冠郁、祈潔、郁婷、馥境、勝堯、佑昀、以真、倩怡、韻倫、孟鴻、柏安、幸佳、穎志、恆毅、可欣等人陪伴我度過了兩年的坎坎坷坷，也讓我的台灣生活充滿了無窮的精彩，更富有了我的人生。

最後,我要特別感謝親愛的父母多年以來對我的照顧與培養,無論是在生活或是精神上,都給予我強力的後盾,使我能專心地在台灣完成學業;感謝我的妻子芝也，在我忙碌、失意的的時候陪伴、鼓勵著我，給予我精神的支柱。

願您們一同分享我這一切喜悅，在今後的人生旅程中一帆風順。

中文摘要

高錳酸鉀首次運用於全氟辛酸在水溶液中的降解研究。全氟辛酸的降解分為分解與脫氟兩部份，超聲波振幅、高錳酸鉀劑量、溶液初始 pH 值及溫度為其反应速率的影響因子。全氟辛酸的分解為擬一階反應，隨著振幅的增加(20μm、40μm 與 60μm)，超聲波輸出能量的提高，其速率常數(K_{1obs})顯著地從 0.0021 上升到 0.0146 min^{-1}。氟元素離子化的過程稱作全氟辛酸脫氟反應，可模擬為零階反應(K_{2obs})。高錳酸鉀的劑量效應說明其分別作為活化劑與氧化劑參與到全氟辛酸的分解與脫氟反應中。在本研究的劑量範圍中，以 $\ln(K_{2obs})$對 $\ln([KMnO_4]_0)$作圖，可得到一條線性回歸線。對於 132μM 的全氟辛酸而言，分解反應與脫氟反應的最佳劑量分別為 3mM 與 10mM。相對於強酸性（pH=2）與中性環境，pH=4 的酸性環境與 pH=11 的強鹼性環境最利於全氟辛酸的降解。將溫度從 30℃ 升至 50℃，全氟辛酸的降解速率有輕微的提升。雖然高溫能有效加速氧化過程，但同時也降低了超聲波的能量輸出。一組高錳酸鉀與雙氧水的對比試驗分別在氬氣、空氣與氧氣的氛圍下進行。曝氬氣能把溶液中的溶解氧掃除，進而把高錳酸鉀-超聲波與雙氧水-超聲波系統的 K_{2obs} 分別提高 1.57 倍與 2.40 倍；而曝氧氣時則將 K_{2obs} 分別降低至 0.72 與 0.51 倍。這是由於溶解氧在超聲波系統中引發的自由基鏈式反應的終止步驟。根據所有得出的實驗數據，本研究提出全氟辛酸在高錳酸鉀-超聲波系統中的分解与脫氟機制。

關鍵字：全氟辛酸，分解，脫氟，高錳酸根，超聲波照射

ABSTRACT

Permanganate was investigated for the first time as an activator for the degradation of perfluorooctanoic acid (PFOA) in aqueous solution. PFOA Degradation, consisted of decomposition and defluorination, were investigated as a function of amplitude of ultrasonic waves, permanganate dosage, pH and temperature in ultrasonic system. The decomposition of PFOA was of pseudo-first order, and the rate constant ($K_{1\mathrm{obs}}$) increased significantly, from 0.0021 to 0.0146 min^{-1}, with raised amplitude (20μm, 40μm and 60μm) which determine the output power of ultrasonic irradiation into medium. Ionization process of fluorine, named PFOA defluorination, could be simulated with pseudo-zero order ($K_{2\mathrm{obs}}$). Dosages effect shown that permanganate act as an activator for PFOA decomposition and oxidant for defluorination. And plotting ln($K_{2\mathrm{obs}}$) versus ln($[KMnO_4]_0$) gave a linear curve in the dosages range studied. For 132 μM initial concentration of PFOA, 3mM and 10mM permanganate is optimal for decomposition and defluorination efficiency, respectively. Reaction solution with an initial pH of 4.0 and 11.0 were most favorable for PFOA degradation activities as compare to highly acidic and neutral condition. Degradation process was observed to be promoted slightly from 30℃ to 50℃, as high temperature would accelerate the oxidation process by permanganate but abate the power output of ultrasonication. A comparative investigation between permanganate and perhydrol under oxygen, air and argon atmosphere, respectively, was carried out to study the atmosphere effect. Aeration with argon gas, which could sweep away dissolved oxygen, improved $K_{2\mathrm{obs}}$ to 1.57 for permanganate-ultrasonic and 2.40 times for perhydrol-ultrasonic system; while aeration with oxygen decreased $K_{2\mathrm{obs}}$ to 0.72 and 0.51 time due to the termination steps induced by oxygen molecules. With experimental results, the mechanisms of PFOA decomposition and defluorination in permanganate-ultrasonic system were proposed, respectively.

Keywords: Perfluorooctanoic acid, Decomposition, Defluorination, Permanganate, Ultrasonic irradiation

CONTENTS

LIST OF FIGURES

LIST OF TABLES

Chapter 1 Introduction

1.1 Research motivation

Perfluorooctanoic acid (PFOA), consist of a hydrophobic group (perfluoroalkyl group) and a hydrophilic group (carboxylate group), is a synthetic, stable perfluorinated carboxylic acid and classified as anionic surfactant. Because of its strong surface-active characteristic, excellent physicochemical stability and high light transparency (Key et al., 1997), since 1940s, PFOA has been widely used as a processing aid (emulsifier) in the production of polytetrafluoroethylene (PTFE) and other fluoropolymers and fluoroelastomers which are used as non-stick coatings on cookware, membranes for waterproof/breathable clothing, electrical wire casing, fire and chemical resistant tubing, and plumbing thread seal tape (Post et al., 2012).

For such wide application, PFOA is not an emerging but common contaminant in surface waters in many regions, such as USA, Canada, Germany, Netherlands, Japan and China with a concentration range of 10^{-1}~10^{4} ng/L (Zareitalabad et al., 2013). What's worse is that PFOA can bioaccumulate and biomagnify through food webs, reaching elevated concentrations in higher trophic level species (Houde et al., 2006). Serum levels of humans reported from industrialized countries around the world are reasonably consistent, with arithmetic means of 2–8 ng/mL (Vestergren and Cousins, 2009). PFOA is a carcinogen, liver toxicant, developmental toxicant and immune system toxicant (Lau et al., 2007); higher concentrations of serum PFOA are also associated with current thyroid disease in the U.S. general adult population (Melzer et al., 2010).

Therefore, the investigation and development of promising treatment technologies is of increasing significance for abating exposure risks of humans and wild life. PFOA is chemically inert due to its strong carbon-fluorine (C-F) bond (Vecitis et al., 2008). Thereby it is very recalcitrant and not removed from drinking water by standard treatment processes such as coagulation, sand filtration, sedimentation, ozonation, or chlorination (Post et al., 2012). In past decade, investigators were striving to study the treatability of PFOA and observed effective degradation under special condition: sonochemical decomposition (Moriwaki et al., 2005; Cheng et al., 2008), Photochemical decomposition (Hori et al., 2007), microwave-hydrothermal decomposition (Lee et al., 2010), and removal by granular activated carbon (Ochoa-Herrera and Sierra-Alvarez, 2008).

Permanganate (MnO_4^-) has attracted much attention due to its strong oxidation capacity and environmental friendliness of avoiding formation of chlorinated DBPs and bromate in chlorination and ozonation processes. Results in many researches showed permanganate could effectively mineralize persistent contaminants, such as hexahydro-1,3,5-trinitro -1,3,5-triazine (RDX) (Albano et al., 2010) and azo dye X-3B (Han et al., 2013). pH, as an operating parameter, determine the oxidation potential (Pe^0) (Walton et al., 1991) and oxidation efficiency by permanganate (Aleboyeh et al., 2009; Olya et al., 2012). However, the oxidized capacity of permanganate for dissolved PFOA still unclear.

Although PFOA might decompose completely as the time goes under ultrasonic irradiation, defluorination efficiency remains undesirable. Here we explore the activated capacity of permanganate in ultrasonic system for elevating the reaction rate of PFOA decomposition and defluorination.

1.2 Research objectives

This study aims to establish a feasible technique by incorporating Sonochemical apparatus and permanganate oxidant to obtain a high decomposition and defluorination rate for PFOA. The objectives of this study are to:

(a) Improve the rate of PFOA decomposition and defluorination by permanganate-ultrasonic (PM-US) system.

(b) Identify the roles of ultrasonic irradiation and permanganate, respectively, for PFOA degradation in PM-US system.

(c) Optimize operation parameters for degradation procedures in PM-US systems, such as $KMnO_4$ dosages, solution pH and temperature.

(d) Investigate the effect of oxygen and inert gases on PFOA degradation rate in PM-US system.

(e) Investigate the effect of co-dissolved heavy metal cations on PFOA degradation rate in PM-US system.

(f) Discuss the reactive kinetics, pathways and mechanisms of PFOA degradation in PM-US system.

1.3 Research content

The framework of this study is shown in Fig.1-1. The dotted arrows are from experimental results to discussions; the solid arrows represent the research sequence; kinetics, intermediates and mechanisms were obtained with all experimental results and discussions.

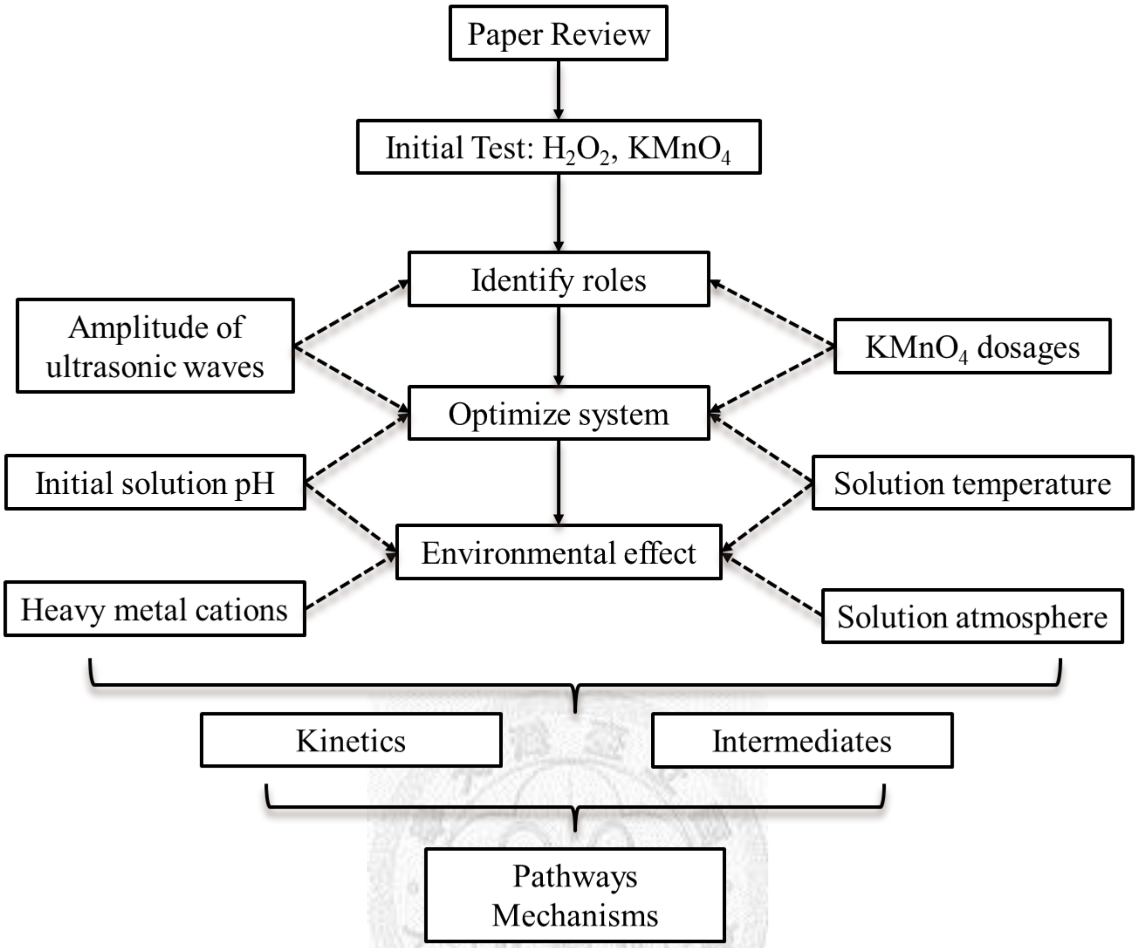

Fig.1-1 The framework of permanganate-ultrasonic system research for PFOA degradation

Chapter 2 Literature Review

2.1 Perfluorooctanoic acid and influencing factors of degradation

Since the 1950s, perfluorinated compounds (PFCs) are produced and widely applied in protective coatings for textile fabrics in the metal industry and production of semi-conductors in the electronics (Zareitalabad et al., 2013). Linear-chain PFCs contained a carboxylic group are named perfluorinated carboxylic acids (PFCAs, $F(CF_2)_nCOO^-$).

Roughly 80% PFCAs had been released into the environment during fluoropolymer manufacture and use resulting in direct contamination (Prevedouros et al., 2005). Table 2-1 showed the historical period of application and the global industry-wide emissions for various PFCA source.

Perfluorooctanoate (PFO) or Perfluorooctanoic acid (PFOA), as one of the PFCAs homologue, containing eight carbon, usually constitute a large proportion of detected PFCs (Prevedouros et al., 2005; Loos et al., 2010). As presented in the last entry of Table 2-1, PFCA emissions from PFO-relevant (PFO/APFO/POSF) sources consisted over 70 percent of total emissions. And the total environmental release of PFO (2700-6200 t) can be estimated as 85% of the total PFCA releases (3200-7300 t). Thus, PFOA is most influential and representative of all PFCs in environment.

Table 2-1 Global Historical PFCA Production and Emissions Summary

Environmental input source	**Historical period**	**Global emissions**	**Percent of emission**
Direct PFCA source			
PFCA manufacture			
PFO/APFO[a]	1951-2012	400-700	10%
PFN/APFN[b]	1975-2012	70-200	3%
Industrial and Consumer Uses			
Fluoropolymer manufacture (APFO)	1951-2012	2000-4000	57%
Fluoropolymer dispersion processing (APFO)	1951-2012	200-300	5%
Fluoropolymer manufacture (APFN)	1975-2012	400-1400	17%
Fluoropolymer processing (APFN)	1975-2012	10-20	0.3%
Aqueous fire fighting foams (AFFF[c])	1965-1974	50-100	4%
Consumer and industrial products	1960-2000	40-200	
Indirect PFCA Sources			
POSF-based products			
PFCA residual impurities	1960-2002	20-130	1%
POSF[d]-based precursor degradation	1960-2002	1-30	0.3%
POSF-based AFFF	1970-2002	3-30	0.3%
fluorotelomer-based products			
PFCA residual impurities	1974-2012	0.3-30	0.3%
fluorotelomer-based precursor degradation	1974-2012	6-130	1%
fluorotelomer-based AFFF	1975-2012	< 1	

[a]APFO = ammonium perfluorooctanoate; [b]APFN = ammonium perfluorononanoate; [c]AFFF = aqueous fire-fighting foam; [d]POSF = perfluorooctylsulfonyl fluoride.

The aqueous pK_a of PFOA was found to be 3.8 ± 0.1 using a standard water-methanol mixed solvent approach (Burns et al., 2008). This constant revealed the acidity of PFOA is weaker than its shorter-chain PFCA homologues. High concentration of PFOA would suppress its pK_a to around 2.3 as the aggregation of perfluorooctanoate formed. In this study of experimental pK_a for PFOA, variation of aqueous pK_a with PFOA concentration can be described by Eq. (2-1) with R^2=0.9.

$$pK_a = -0.1278\ [\mathrm{PFOA}] + 3.8437 \tag{2-1}$$

Extrapolation of the Antoine equation to 25 ℃ for $CF_3(CF_2)_6COOH$ results in an estimated vapor pressure of 4.2 Pa (Kaiser et al., 2005). The vapor pressure for $CF_3(CF_2)_6COO^-$ is expected to be negligible, although it has not been measured (Prevedouros et al., 2005). According to the results presented in a study about Henry's law constant (K_H) of $CF_3(CF_2)_6COOH$ at 298 K in aqueous sulfuric acid solutions (Kutsuna and Hori, 2008), the K_H ($mol{\cdot}dm^{-3}{\cdot}atm^{-1}$) of $CF_3(CF_2)_6COOH$ would augment with increased H_2SO_4 dosages followed by $CF_3(CF_2)_6COO^-$ transformed to $CF_3(CF_2)_6COOH$.

PFOA is had been found in the blood serum of humans since 1981, but not evidence of PFOA transformation has been reported (Key et al., 1997). However, data collected from researches of PFOA mammalian toxicology via repeat-dose studies and dose-response curve showed substantial hepatotoxicity, developmental toxicity, immunotoxicity, hormonal effects and underlying biochemical effects on genes and biotransformation (Lau et al., 2007).

Such toxic, carcinogenic, and widely distributed contaminant is nondegradable by most commonly used treatments such as biological method, ozonation, or Fenton's oxidation, due to its strong energy of carbon-carbon (C-C) energy (average 410 kJ mol^{-1}) and C-F bond (average 530 kJ mol^{-1}). Therefore, until present time, great efforts have been taken into develop methods to decompose this pollutant into harmless species. It has been reported that PFOA can be degradable under special condition, sonochemical decomposition (Moriwaki et al., 2005), Photochemical decomposition (Hori et al., 2004; Wang et al., 2008; Tang et al., 2012), chemical oxidation by periodate (Cao et al., 2010) , persulfate (Hori et al., 2005; Lee et al., 2009) or peroxidase-mediated hydrogen peroxide (Colosi et al., 2009), reduction by iodide ion (Qu et al., 2010) and β-Ga_2O_3 (Zhao and Zhang, 2009), and electrochemical decomposition of PFOA in $NaClO_4$ solution (Ochiai et al., 2011). Ferric (Wang et al., 2008) and ferrous ion (Lee et al., 2010) had been reported as an activator for PFOA degradation. Parameters, rate constants and efficiencies of PFOA degradation in various system were summarized in Table 2-2.

Although PFOA seemed to be un-degradable in Fenton system by the result of Fenton reactions (degradation of PFOA was not observed (Moriwaki et al., 2005) when the Fenton reagents (0.2mM, Fe^{2+}/ H_2O_2 molar ratio = 1:1) were added into the PFOS and PFOA solution (0.02mM)), it was found that PFOA could be efficiently degraded in the UV–Fenton system, producing fluoride ions and short-chain perfluorinated carboxylic acids (Tang et al., 2012). Two kinds of radical species, •OH and HO_2・, would generate in a Fenton system. Tertiary butyl alcohol (TBA), as an effective scavenger of •OH, and benzoquinone (BQ), only reacting with HO_2・ radicals, can used to check reactive radical species for PFOA degradation. For now, applied feasibility of H_2O_2 in sonochemical system is still unknown for PFOA.

Table 2-2　Summaries of PFOA degradation in various systems

System	Regent	Power (W)	Time (min)	$[\mathrm{PFOA}]_0$ (μM)	V (mL)	K^1 (Min^{-1})	E^1 %	E^2 %	Notes
UV^3		200	4320	29.6	22		89.5	33.6	Hori et al., 2004
$\mathrm{UV+S_2O_8^{2-}}$	$\mathrm{S_2O_8^{2-}}$: 50 mM	200	240	29.6	22		100	59.1	Hori et al., 2005
US^4 200kHz		200	60	24.15	60	0.0155	63		Moriwaki et al., 2005
$\mathrm{UV+\ Fe^{3+}}$ 254nm	$\mathrm{Fe^{3+}}$: 50 μM	23	240	48	500	0.0065	78.9	38.7	Wang et al., 2008
$\mathrm{UV+IO_4^-}$ 254nm	$\mathrm{IO_4^-}$: 0.5 mM	23	120	10		0.0097	70	17	Cao et al., 2010
UV+Fenton 254nm	$\mathrm{H_2O_2}$: 30 mM $\mathrm{Fe^{2+}}$: 2 mM	9	60	20	200		87.9	35.8	Tang et al., 2012
peroxidase + $\mathrm{H_2O_2}$	$\mathrm{H_2O_2}$: 750 μM	0	360	850	6	0.003	68	0.83	Colosi et al., 2009
$\mathrm{MW^5+\ S_2O_8^{2-}}$ 90℃	$\mathrm{S_2O_8^{2-}}$: 5 mM	70	120	253.8	50	0.0055	47.4		Lee et al., 2009
$\mathrm{MW+\ S_2O_8^{2-}}$ +ZVI, 90℃	$\mathrm{S_2O_8^{2-}}$: 5 mM ZVI: 3.6 mM	70	120	240.7	50	0.0146	67.6	22.5	Lee et al., 2010
$\mathrm{UV+Ga_2O_3}$ 254nm	$\mathrm{Ga_2O_3}$: 0.5 g/L	15	180	96.6	100		39	16	Zhao et al., 2009
$\mathrm{UV+I^-}$ 254nm	$\mathrm{I^-}$: 0.3 mM	15	360	25	740		93.9	76.8	Qu et al., 2010
$\mathrm{EC^6+ClO_4^-}$ $0.15\ \mathrm{mA/cm^2}$	$\mathrm{ClO_4^-}$: 10 mM	1	600	8000	300		45.8	2.1	Ochiai et al., 2011

^{1}K = rate constant of PFOA decomposition, ^{1}E = efficiency of PFOA decomposition, ^{2}E = efficiency of PFOA defluorination, ^{3}UV = ultraviolet system, ^{4}US = ultrasonic system, ^{5}MW = microwave system, and ^{6}EC = electrochemical system.

Except Fenton reaction, ferrous ion was utilized as well in sonochemical decomposition of another pollutants, such as 1,4-dioxane (Beckett and Hua, 2003). Ferric ion also showed significant enhancement on the photochemical decomposition of PFOA (Wang et al., 2008) while Cu^{2+} improved slightly.

In one research about the effect of O_2 on OH generation in DC corona discharge, the results showed that the formation of •OH may be inhibited with the increasing amounts of O_2 molecules. So we can assume that the sonochemical decomposition rate of PFOA may be reduced by the presence of O_2 molecule in the solution. The presence of O_2 also slow or inhibit most radical reactions by forming the R-O-O• radical, which is more stable than other radicals:

$$R \cdot + O_2 \rightarrow R\text{-}O\text{-}O \cdot \tag{2-2}$$

On the other hand, a combined process of ozonation and sonolysis is shown to substantially recover the rate loss for PFOA in landfill groundwater (Cheng et al., 2008). But replacing argon with either oxygen or an oxygen/ozone mix gas has no significant effect on the sonochemical kinetics of PFOA in Milli-Q water.

2.2 Permanganate and influencing factors of oxidation

Permanganate has been investigated to capable of oxidizing various persistent organic compounds in water (Walton et al., 1991; Aleboyeh et al., 2009; Albano et al., 2010; Olya et al., 2012; Han et al., 2013) and successfully applied in the drinking water and wastewater treatment industries for oxidation of organic contaminants including halogenated compounds with a long history (Siegrist et al., 2001). Table 2-3 showed the properties and characteristics of potassium permanganate.

Table 2-3 Properties and characteristics of potassium permanganate

Property	Value and/or comments
Molecular formula	$KMnO_4$
Molecular weight	158.04 g/mol
Form and feature	Dark purple solid with metallic luster, sweetest astringent taste, odorless, granular crystalline, oxidizer
Solubility in distilled water:	
0℃	27.8 g/L
20℃	65.0 g/L
40℃	125.2 g/L
60℃	230 g/L
Incompatibilities	Avoid contact with acids, peroxides, and all combustible organics or readily oxidizable materials

The stoichiometry and kinetics of conyaminants oxidation by permanganate can be quite complex as there are various reactions in which manganese participate due to its multiple mineral forms and valence states (+2,3,4,5,6,7) owning different oxidation potential. According to the stoichiometric equations shown in Eqs. (2-3)-(2-6) (Yan and Schwartz, 1999), $[H^+]$ determines the reactivity of permanganate resulting in different redox pathways and redox potential (Pe^0) of permanganate increase with pH decline. Under highly acidic condition (pH<3.5), one permanganate undergoes a five-electron exchange (Eq. (2-3)) with $Pe^0 = +25.5$. From pH=3.5 to 12, one permanganate undergoes a three-electron exchange via Eq. (2-4) in acidic pH conditions and Eq. (2-5) in neutral or alkaline condition completed with $Pe^0 = +28.7$ and +9.9, respectively. Under highly alkaline (pH>12) condition (Eq. (2-6)), one-electron exchange take place and Pe^0 is only +9.5. MnO_2, as the reduction products, also own oxidation capacity under acidic condition with a considerable $Pe^0 = 20.8$ (Morel and Hering, 1993) via Eq. (2-7).

$$\frac{1}{5}MnO_4^- + \frac{8}{5}H^+ + e^- = \frac{1}{5}Mn^{2+} + \frac{4}{5}H_2O \qquad Pe^0 = +25.5 \qquad pH < 3.5 \qquad (2\text{-}3)$$

$$\frac{1}{3}MnO_4^- + \frac{4}{3}H^+ + e^- = \frac{1}{3}MnO_2 + \frac{2}{3}H_2O \qquad Pe^0 = +28.7 \qquad 3.5 < pH < 12 \qquad (2\text{-}4)$$

$$\frac{1}{3}MnO_4^- + \frac{2}{3}H_2O + e^- = \frac{1}{3}MnO_2 + \frac{4}{3}OH^- \qquad Pe^0 = +9.9 \qquad 3.5 < pH < 12 \qquad (2\text{-}5)$$

$$MnO_4^- + e^- = MnO_4^{2-} \qquad Pe^0 = +9.5 \qquad pH > 12 \qquad (2\text{-}6)$$

$$\frac{1}{2}MnO_2(s) + 2H^+ + e^- = \frac{1}{2}Mn^{2+} + H_2O \qquad Pe^0 = +20.8 \qquad (2\text{-}7)$$

The greatest oxidation potential that permanganate own is +28.7 under acidic condition around pH=3.5. This is lower than that of many other oxidants including perhydroxyl radical (+28.9), hydrogen peroxide (+30.1), ozone (+35.0), atomic oxygen (+40.9), hydroxyl radical (+47.32) and fluorine (+51.2). Hydrogen peroxide (as the Fenton regent) (Tang et al., 2012), ozone (Cheng et al., 2008) had been observed to catalyze PFOA degradation under ultraviolet and ultrasonic irradiation, respectively. And permanganate has still unclear effect on PFOA degradation.

Temperature is also a significant factor influencing oxidative capacity. Arrhenius equation presented a linear relation between reciprocal of temperature (T, K) and Napierian logarithm of rate constant (*k*) of oxidation with permanganate (Eq. (2-8)).

$$\ln(k) = \ln(A) - E_a/RT \quad (2\text{-}8)$$

Where A is a constant with unit same with k. This linear curve give $-(E_a/R)$ as the slope and E_a as the activation energy. The activation energies were +29.5 kJ/mol and +28.8 kJ/mol for the oxidation of dichlorvos and microcystins, respectively, with permanganate (Liu et al., 2009).

2.3 Ultrasonic irradiation and influencing factors of ultrasonication

An ultrasonic treatment apparatus comprises at least one hand piece, a plurality of probe, and an ultrasonic drive device. The hand piece has an ultrasonic oscillation device for generation ultrasonic vibration generated by the hand piece. And the ultrasonic drive device is connected to the hand piece, for driving the ultrasonic oscillation device (Sakurai et al., 1998). The amplitude of ultrasonic waves, external static pressure, temperature and viscosity of medium would influence, either individually or in combination, on the amount of power transferred into a liquid medium during ultrasonication (Raso et al., 1999).

Ultrasonic apparatus is effective for the removal of contaminants with high Henry's Law constants that partition into the vapor phase of the bubble or for surfactants that partition to the air-water interface (Vecitis et al., 2008). Average temperature raise to 4000 K in internal vapor phase and 600-1000 K on bubble-water interface via transient collapse of aqueous cavitation bubbles under ultrasonication. The chemical effects of ultrasound for surfactants are attributed to cavitation, which is accompanied by the conditions of high temperature and high pressure:

(1) Interiors of collapsing cavities:

-temperatures of several thousand degrees

-pressures of hundreds of atmospheres

-Water vapor is pyrolyzed to •OH radicals and •H

-gas phase pyrolysis and combustion reactions of volatile substances

-pyrolysis or combustion of volatile solute molecules take place.

(2) Interfacial regions:

-temperature is lower, but a high temperature with a high gradient is still present.

-Locally condensed OH radicals

-Thermal decomposition and reaction with •OH radicals and •H

Therefore, bubble is a significant part of ultrasonic irradiation. According to the research of surfactants sonolysis in aqueous solutions (Yim et al., 2002), the results suggest that the surfactant, which is non-volatile and a water-soluble solute, exists with a high accumulation ratio in the interfacial region of the cavitation bubbles and is degraded by the thermal reaction as well as the hydroxyl radical oxidation. Thus, we can expect that the growth in number of bubbles may improve the sonochemical decomposition and defluorination rate of PFOA.

According to several investigations in the past, ultrasonic apparatus is a good choice to degrade PFOA (Moriwaki et al., 2005; Cheng et al., 2008; Vecitis et al., 2008). When operating at 200W, the average power introduced to the reactor was 3 W/cm^2, and the temperature of the solution was kept at 20℃ by a cooling water bath during sonication, 63% of PFOA (initial concentration was 0.024mM) was decomposed (60min) under an air atmosphere (Moriwaki et al., 2005). Sonochemical degradation of organic pollutants via reaction with OH radicals, which are formed from water pyrolysis in the collapsing hot bubbles, and the degradation proceeds of volatile or hydrophobic pollutants not only via OH radical reaction inside or in the vicinity of the collapsing bubbles. Moriwaki suggest that most of the PFOA molecules are pyrolyzed at the interfacial region and would undergo shortening of the perfluorocarbon chain caused by repetition of the $-COO^-$ dissociation and the oxidation of the generated ions or radicals of the perfluorocarbon. The decomposition and defluorination efficiencies would be improved considerably via combining ultrasonic apparatus and ultraviolet (Sri Chandana Panchangam, 2009) or electrochemical (Zhao et al., 2013) system. Parameters and efficiencies of PFOA decomposition and defluorination in ultrasonic-relevant systems were presented in Table 2-4.

Table 2-4 Parameters and efficiencies of PFOA decomposition and defluorination in ultrasonic-relevant systems

System	Power of US (W)	Frequency of US	Time (min)	$[PFOA]_0$ (μM)	V (mL)	K^1 (Min^{-1})	E^1 %	E^2 %	Notes
US^3	200	200kHz	60	24.15	60	0.0155	63		Moriwaki et al., 2005
US	150	612kHz	140	0.24	600	0.047			Cheng et al., 2008
US	150	618kHz	120	12	600	0.036	100	100	Vecitis et al., 2008
US+UV^4 (16W, 254nm)	500	40kHz	480	120	3000	0.0022	64	5.3	Panchangam et al., 2009
US+EC^5 20 mA/cm^2	50	33kHz	300	241.5		0.0087	91.3	80.1	Zhao et al., 2013

^{1}K = rate constant of PFOA decomposition, ^{1}E = efficiency of PFOA decomposition, ^{2}E = efficiency of PFOA defluorination, ^{3}US = ultrasonic system, ^{4}UV = ultraviolet system, ^{5}EC = electrochemical system.

Both organic matrix and inorganic matrix in environmental would influence PFOA ultrasonication. The pseudo-first order rate constant for the sonochemical degradation in the landfill groundwater is reduced by 56% relative to Milli-Q water for PFOA, primarily due to the presence of other organic constituents (Cheng et al., 2008) by competitive adsorption onto the bubble-water interface or by lowering the average interfacial temperatures during transient bubble collapse events. Volatile organic compounds (VOCs) are identified as the primary cause of the sonochemical rate reduction for PFOS and PFOA in landfill groundwater, whereas the effect of dissolved natural organic matter (DOM) is not significant. Sonochemical rate constants for PFOA increase steadily as the concentration of $NaClO_4$ increases (Cheng et al., 2009).

Aeration was used primarily and significant operating methods for wastewater treatment. The basic purpose of aeration is to improve water quality for subsequent usage (Rajenden, 2000). The saturated argon gas, as can be learned from comparison experiments under different atmosphere (gas components), accelerated the sonochemical degradation of PFOA with complex reasons (Moriwaki et al., 2005). The follow equations show the possible radical reactions in sonolysis water in argon atmosphere or oxygen atmosphere (Nagata et al., 1996).

Argon atmosphere:

$$H_2O \rightarrow H\cdot + \cdot OH \qquad (2\text{-}6)$$

$$H\cdot + H\cdot \rightarrow H_2 \qquad (2\text{-}7)$$

$$\cdot OH + \cdot OH \rightarrow H_2O_2 \qquad (2\text{-}8)$$

$$H\cdot + \cdot OH \rightarrow H_2O \qquad (2\text{-}9)$$

Oxygen atmosphere:

$$H\cdot + O_2 \rightarrow HO_2\cdot \tag{2-10}$$

$$HO_2\cdot + HO_2\cdot \rightarrow O_2 + H_2O_2 \tag{2-11}$$

$$HO_2\cdot + \cdot OH \rightarrow O_2 + H_2O \tag{2-12}$$

The sono-ozone process has been shown to enhance the OH radicals production rate (Cheng et al., 2008). OH radicals will react with VOCs present in the bubble vapor phase at a much faster rate than the thermal dissociation of these molecules and will increase their mineralization rates. The rapid destruction of VOCs will reduce their negative impact on interfacial temperatures during bubble collapse. This result also indicated the significance of interfacial region for sonochemical decomposition of PFOA.

For the acidification experiments (Cheng et al., 2009), the groundwater was acidified to pH 3.9 by HCl to convert bicarbonate to carbon dioxide, which was then removed from solution by bubbling with argon. The sonochemical degradation rates are enhanced to 104.4% for PFOA relative to the Milli-Q rates. The experiments suggest that bicarbonate is primarily responsible for the reduction in PFOX sonochemical kinetics in the groundwater in this study. The same effects of bicarbonate on sonochemical degradation rates were found in the research of sonochemical decomposition of 1,4-dioxane (Beckett and Hua, 2003).

Chapter 3 Materials and methods

3.1 Experimental chemicals and apparatus

3.1.1 Experimental chemicals

1. Perfluorooctanoic acid (PFOA), $C_7F_{15}COOH$: 96%, Sigma-Aldrich (St. Louis, Mo, USA).
2. Perfluoroheptanoic acid (PFHpA), $C_6F_{13}COOH$: 98%, Alfa Aesar.
3. Undecafluorohexanoic acid (PFHeA), $C_5F_{11}COOH$: 97%, Fluka (Buchs, Switzerland)
4. Perfluoropentanoic acid (PFPeA), C_4F_9COOH: 97%, Alfa Aesar.
5. Heptaflurobutyric acid (PFBA), C_3F_7COOH: 99%, Alfa Aesar.
6. Pentafluoropropionic acid (PFPrA), C_2F_5COOH: 97%, Fluka (Buchs, Switzerland).
7. Trifluoroacetic acid (TFA), CF_3COOH: Riedel-de Haën (Germany).
8. Potassium permanganate, $KMnO_4$: 99.0%, J. T. Baker (USA).
9. Sulfuric acid, H_2SO_4: 98.08 g/mol, 95-97%, Fluka (Germany).
10. Sodium hydroxide, NaOH: 40 g/mol, 97%, Nacalai Lesque (Japan).
11. Tert butyl alcohol (TBA), $(CH_3)_3COH$: 74.12 g/mol, 99.7%, J.T.Baker (USA).
12. Hydrogen peroxide, H_2O_2: 34.01 g/mol, 30% (w/w), 1.11 g/cm^3, Scharlau (Spain).
13. Iron (II) sulfate heptahydrate, $FeSO_4·7H_2O$: 278.01 g/mol, 99%, Sigma-Aldrich (Germany).
14. Copper (II) sulfate pentahydrate, $CuSO_4·5H_2O$: 249.68 g/mol, Crown (Japan).

15. Iron (III) nitrate nonahydrate, $Fe_2(SO_4)_3 \cdot 9H_2O$, 404 g/mol, 99%, Merck (Germany).
16. Sodium carbonate, $NaCO_3$: 105.99 g/mol, 99.9%, Merck (Germany).
17. Sodium hydrogen carbonate, $NaHCO_3$: 84.01 g/mol, 99.7%, Merck (Germany).
18. Boric acid, H_3BO_3; 61.83 g/mol, 99.5%, Merck (Germany).
19. Acetonitrile, CH_3CN: 41.05 g/mol, 99.9%, J. T. Baker (China).
20. Milli-Q (deionized, DI) water: 18.2 MΩ·cm at the first day and 25℃, produced by Merck Millipore.

3.1.2 Experimental apparatus

1. Cylindrically jacketed glass reactor (inside diameter = 8 cm); It was used for containing reaction solutions and the cooling water went through its jacket layer.

Fig. 3-1 Cylindrically jacketed glass reactor

2. Ultrasonic apparatus, Branson Lpt (continuous mode, 150W, 40 kHz): It consisted of an ultrasonic drive device to set amplitude of ultrasonic waves, a hand piece contains an ultrasonic oscillator for generating vibration, and a probe (D = 3.5 cm, L = 9.0 cm) for transmitting the energy of vibration into solution.

Fig. 3-2 Ultrasonic oscillator equipped with a probe

3. Magnetic stirring apparatus, Fargo MS-90: It was used for mixing reaction solution throughout the ultrasonication time.
4. Cooling water circulator: It was used to maintain the temperature of reaction solution
5. Aeration ring (outer diameter = 8 cm): It was used to disperse bubbles with 20 pores on the ring.

Fig. 3-3 Aeration ring

6. pH meter, HTC-201U, Taiwan: It was used to monitor pH values of reaction solution when sampling.
7. Refrigerated centrifuge (z32 HK, 50/60Hz, 1200W), Hermle Labortechnik GmbH z32 HK, Germany: It was used to separate precipitate and liquid phase of samples.
8. Pipette: They were used for prepare stock and reaction solution

   10~100 μL, Micropipette, Solid calibration, Calibra 822

    100~1000 μL, Transferpette, Socopex Acura 825, Swiss
    1~5 mL, Transferpette, Brand, Germany
    1~10 mL, Transferpette, Brand, Germany

9. Syringe (with needle), 3 mL, Terumo, Belgium.
10. Filter (PTEE), 13 mm*0.22 μM, China: It was used for syringe.
11. Graduated pipette (plastic), 3 mL, α-plus, Taiwan: It was used for collected sample from reactor.
12. Sample vial (with 8 mm septa), 0.5 mL, Sun-Sri, USA.
13. Microcentrifuge tube, 1.5 mL, Spain.
14. Reciprocal shaker bath, BT350.
15. High-performance liquid chromatography (HPLC), Dionex, Ultimate 3000, USA: It was equipped with an Agilent column (Eclipse XDB-C18, 5 μm, USA) for chromatographic separation of analytes, and a set of electrochemical detector and anion self-regenerating suppressor (Dionex AMMS 300, 2 mm, USA) for conductivity measurement.
16. Ion chromatograph (IC), Dionex, Ics-3000: It was equipped with an automatic sample injector, a guard column (Ion Pac As4a Guard Column, Dionex), a separation column (Ion Pac As4a-SC Analytical Column, Dionex), and a conductivity detector with a suppressor device.
17. Ultraviolet-visible spectrometer, Genesys 10S, Thermo Fisher Scientific, USA.
18. Energy Dispersive Spectrometer

3.2 Experimental methods

3.2.1 Ultrasonication methods

As presented in Fig.3-4, ultrasonic irradiation of PFOA aqueous solution was carried out in a cylindrically jacketed glass reactor mounted on a magnetic stirring apparatus. Designed mass of $KMnO_4$ powder or volume of perhydrol, and volume of PFOA stock solution (1000mg/L) were used to prepare 500mL reaction solution (initial concentration of PFOA is 132μM). The ultrasonic apparatus fixed to 150W and 40 kHz, was operated at continuous mode. The probe was inserted into solution 5.8 cm during ultrasonication. Cooling water inflow from the bottom inlet and outflow through the top outlet. 10 min sampling interval and 120 min reaction time were adopted throughout this study. pH and temperature of the solution were monitored timely by pH meter when sampling.

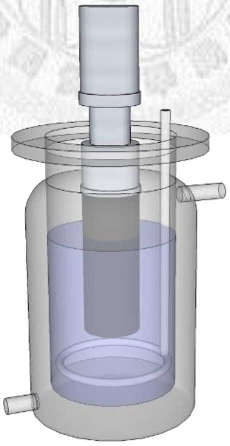

Fig. 3-4 Ultrasonication methods

3.2.2 Parameters variations

Amplitude of ultrasonic waves could be set by ultrasonic drive device. Maybe due to the bad condition of energy transfer efficiency, error would occur and ultrasonic device would crash when amplitude were set above 60μm. So we set amplitude of 20μm, 40μm and 60μm to study its effect. KMnO4 dosages were designed to be 1, 3, 6, 10 and 20mM, respectively. pH were adjusted with 1.8mol/L H_2SO_4 and 0.05mol/L NaOH solution at 2, 3, 4, 5, 7, 10 and 11 before ultrasonication. The temperature of the solution were kept at 30±1℃, 40±1℃and 50±1℃by a cooling water circulator during ultrasonication.

3.2.3 Aeration methods

Nitrogen gas or oxygen gas, as need, was bubbled into solution along with the reactions, A self-designed aeration ring, suited with inner chamber of reactor, was inserted into solution and fixed to the bottom to disperse bubbles at the flow rate of 500 cc/min.

3.2.4 Complexes tests

Fe^{2+}, Cu^{2+} and Fe^{3+} were selected as typical heavy-metal cations for the investigation of complex formation between heavy-metal cations and PFOA. 0.01, 0.05, 0.1, 0.2, 0.5 and 1mM of the three heavy-metal cations were added into 264μM PFOA solution, respectively. All co-dissolved solution were shaken for stabilization in a water bath operated in 30℃ and 150 rpm for 2 hr. 0.2mM dosage of three heavy-metal cations were added into PM-US system for experiments of complex effect on PFOA degradation.

3.3 Sample preparation and analysis

3.3.1 Sample preparation

All samples in this study (mono-ultrasonic system, permanganate-ultrasonic system, perhydrol-ultrasonic system and complex tests) were prepared via a standard process. 1mL samples were collected by plastic straws and placed in a microcentrifuge tube followed by a centrifugation of 8000rpm, 10℃ and 20min. 0.5mL liquid supernatant from centrifugation were transferred by Syringes equipped with filters into the 0.5mL sample vials suited for autosampler in HPLC and IC.

3.3.2 Analysis of PFOA concentration

The concentration of PFOA were analyzed by a high-performance liquid chromatography (HPLC). The mobile phase is 70% acetonitrile and 30% Na_3BO_4 solution at the flow rate of 0.3 ml/min (Lee et al., 2010). The limits of detection (LODs), based on a signal-to-noise (S/N) ratio of 3 and 50 μL injection, were 0.33 mg/L for PFOA.

3.3.3 Analysis of intermediates and final products of PFOA degradation

The concentration of PFPrA, TFA and fluoride ion was measured with an ion-chromatograph (IC) system. The mobile phase of IC was an aqueous solution containing $NaHCO_3$ (1.7 mM) and Na_2CO_3 (1.8 mM) at the flow rate of 2 mL/min. The limits of detection (LODs), based on a signal-to-noise (S/N) ratio of 3 and 50 μL injection, were 0.22 mg/L, 0.15 mg/L and 0.024 mg/L for PFPrA, TFA and fluoride ion, respectively.

3.3.4 Analysis of permanganate and its reduction products

The concentration of permanganate was analyzed using UV-Vis spectrometer in the wavelength range of 200nm to 800nm with a scan speed of “fast” and an interval of 1.0 nm. Brown precipitates remained in microcentrifuge tube (3.3.1) were the reduction products of permanganate. Scanning Electron Microscope and Energy Dispersive Spectrometer were utilized to analyze the precipitate components via the results of elements ratio.

Chapter 4 Results and discussions

4.1 Kinetics of PFOA decomposition and defluorination in permanganate-ultrasonic system

$KMnO_4$, as a strong oxidant for treatment of organic contaminants, performed an activation part effectively for PFOA decomposition and defluorination. The effects of applying $KMnO_4$ on PFOA (132μM) degradation under ultrasonic irradiation at 30℃ were shown in Fig. 1. The addition of 10 mM $KMnO_4$ to the PFOA solution, without US at 30℃, resulted in slight decomposition efficiency (5.1%) for 120 min, and no final product (fluoride ion) was detected that lasted for 3 day. In mono-US system without any oxidants at 30℃, PFOA decomposed 29.6% and 7.7% defluorination efficiency were obtained for 120 min. By adding 10 mM $KMnO_4$ to the PFOA solution in ultrasonic system operated at 30℃, the decomposition and defluorination efficiency of PFOA increased considerably. After two hour ultrasonication, PM-US system achieved 84.3% for PFOA decomposition efficiency and 63.1% for defluorination efficiency. As it is shown in Fig.4-1, decomposition of PFOA and yield of fluoride ions (defluorination) could simulated with the pseudo-first order kinetics and pseudo-zero order, respectively. Therefore, the reaction rate of PFOA decomposition and defluorination was determined using Eq.(4-1) and Eq.(4-2), respectivly.

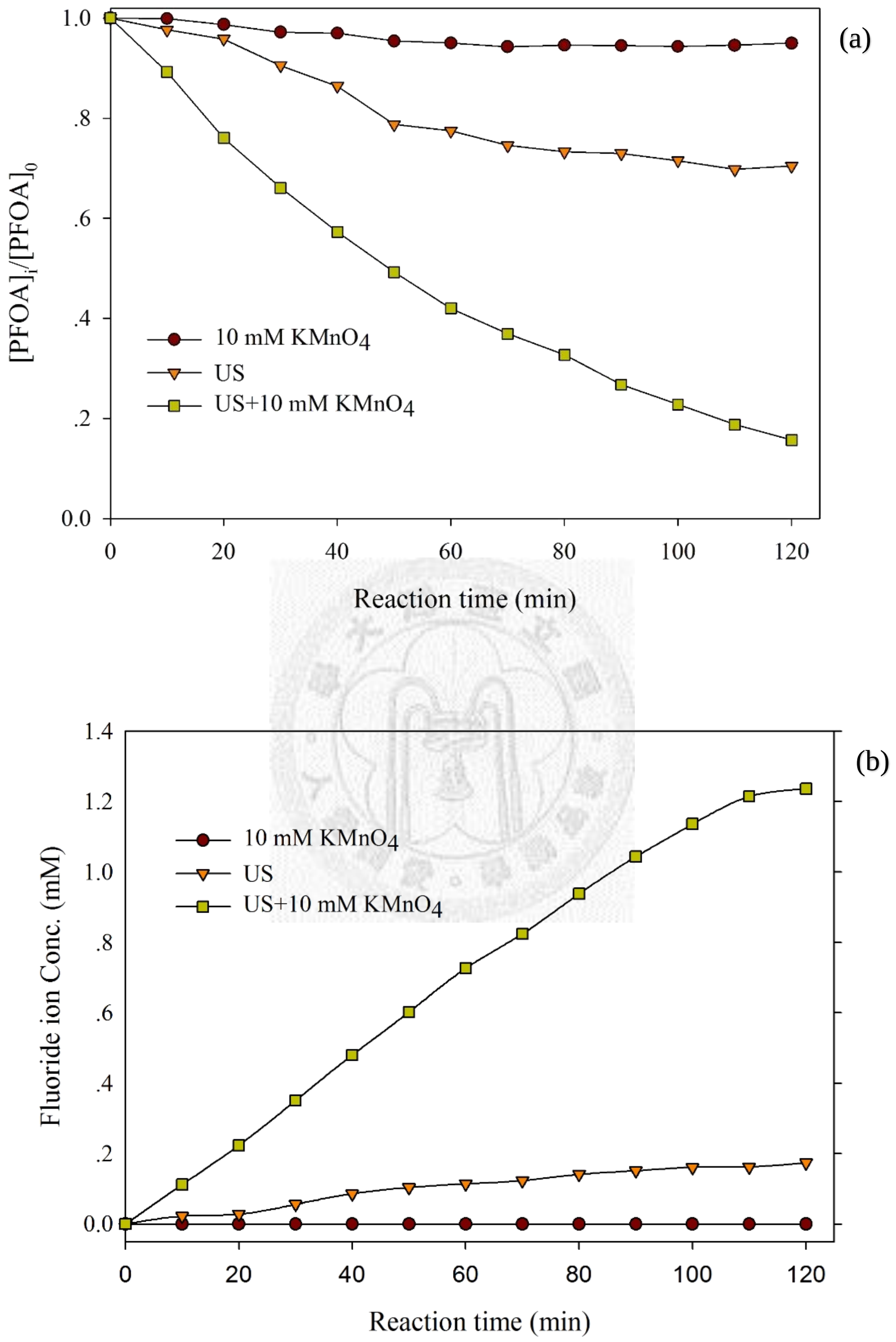

Fig. 4-1 Decomposition (a) and defluorination (b) of PFOA (132 μM) in mono-permanganate (10 mM), mono-ultrasonic (60μm, 150W, 40kHz) and permanganate-ultrasonic system with initial solution pH=4 at 30℃.

$$r_1 = -\frac{d[\mathrm{PFOA}]_i}{dt} = K_{1\mathrm{obs}} \cdot [\mathrm{PFOA}]_i \tag{4-1}$$

$$r_2 = \frac{d[\mathrm{F}^-]_i}{dt} = K_{2\mathrm{obs}} \tag{4-2}$$

Where r_1 and r_2 are the rate of PFOA decomposition and defluorination, $K_{1\mathrm{obs}}$ (min^{-1}) and $K_{2\mathrm{obs}}$ ($\mathrm{mM \cdot min}^{-1}$) are the rate constant of PFOA decomposition and defluorination, resectively. $[\mathrm{PFOA}]_i$ (μM) and $[\mathrm{F}^-]_i$ (mM) are the concentration of PFOA and fluoride ions at time t. All rate constants of PFOA decomposition ($K_{1\mathrm{bos}}$) and defluorination ($K_{2\mathrm{obs}}$) under different reaction conditions in this study were presented in Table 4-2.

4.2 Permanganate consumption and reduction products in permanganate -ultrasonic system

Effects of co-dissolved PFOA, intermediates (perfluorocarboxylic acid with two to seven carbon, PFCAs) and final products fluoride on absorbance of permanganate were tested and presented in Fig.4-2. It revealed that other components in PM-US system would not influence the UV-Vis spectrum of permanganate. Therefore, UV-Vis spectrum is a feasible method for permanganate quantification in PM-US system.

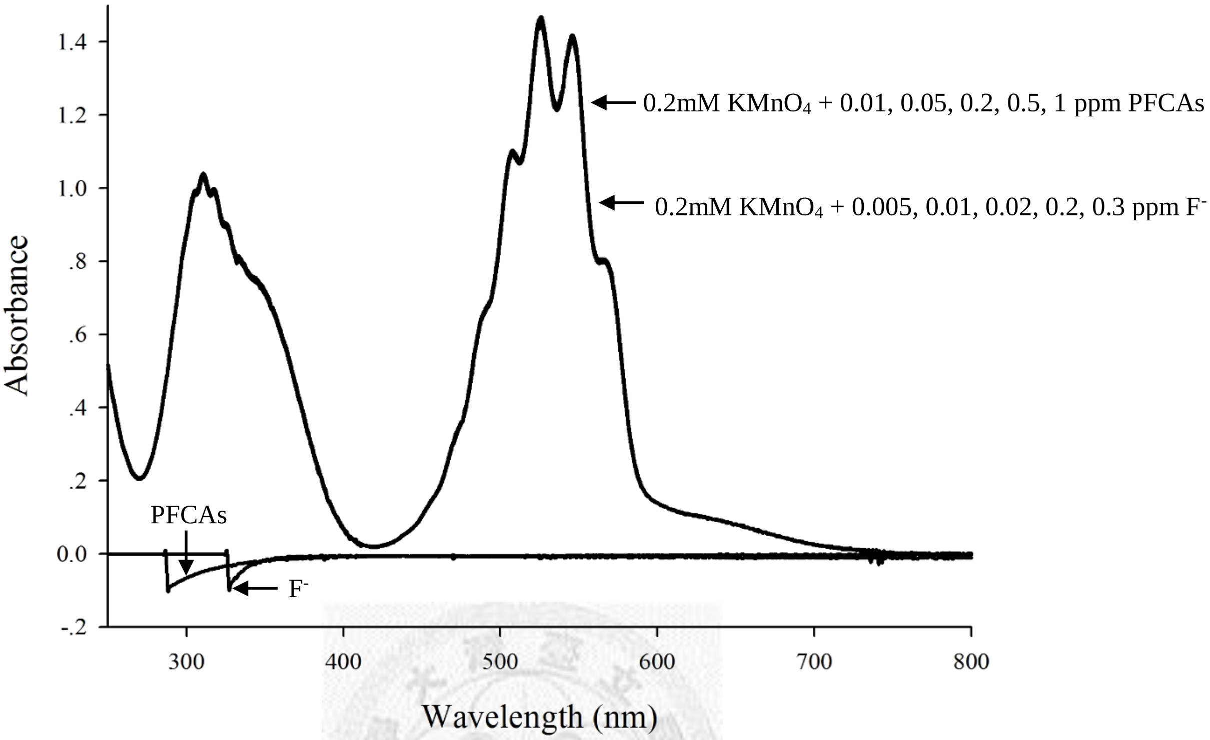

Fig. 4-2 UV-Vis spectrum of single or multiple components solution of $KMnO_4$, PFCAs and fluoride.

In order to quantify permanganate accurately and precisely, peak wavelength 526nm was adopted as detection wavelength and absorbance of calibration curve is controlled under 1. This absorbance limit carried out the concentration range of permanganate calibration solution (Fig.4-3). The samples from PM-US system throughout this study were diluted into this concentration range.

As presented in Fig.4-4, permanganate concentration decreased slightly with varied permanganate dosages. This was due to the dosages are overdosed for initial PFOA concentration (23, 46, 76 and 152 times, respectively). More interpretations would present in next section. For now, we have not observed quantitative relevance between permanganate consumption and PFOA decomposition or defluorination.

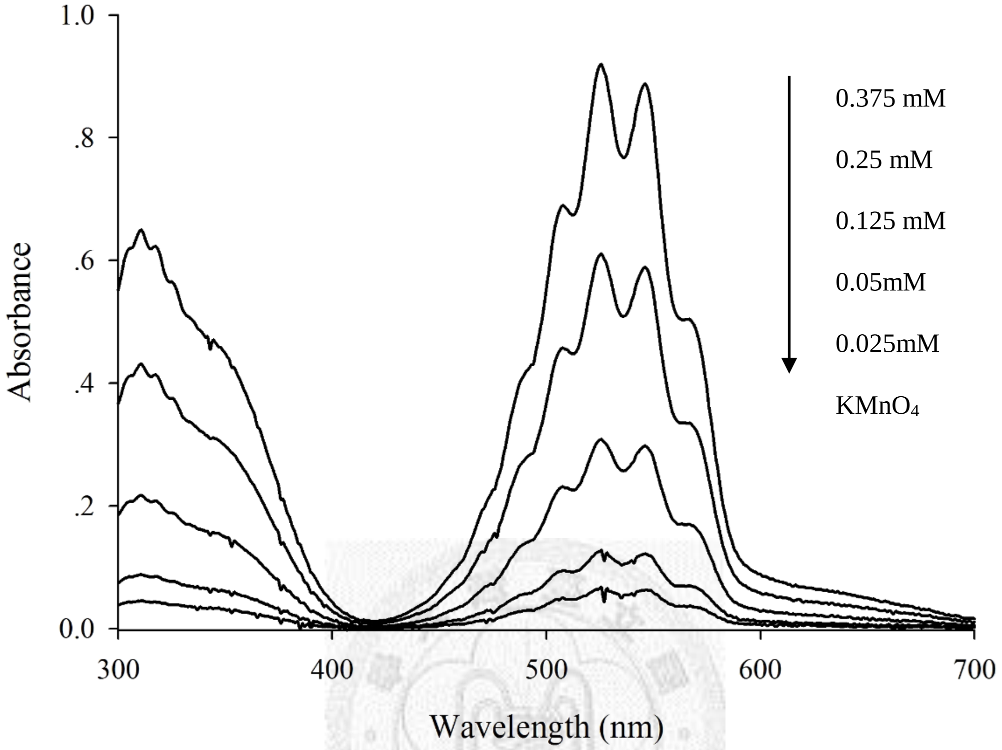

Fig. 4-3 UV-Vis spectrum of $KMnO_4$ solutions with increased concentration

The precipitate products increased apparently during ultrasonication and were collected via centrifugalization of reaction solution in PM-US system. Table 4-1 and Fig.4-5 are the physicochemical analysis results of precipitate products. As elements ratio, analyzed by Energy Dispersive Spectrometer, of oxygen-to-manganese of is roughly equal to 2 (Table 4-1), MnO_2 is considered as reduction products of permanganate in PM-US system.

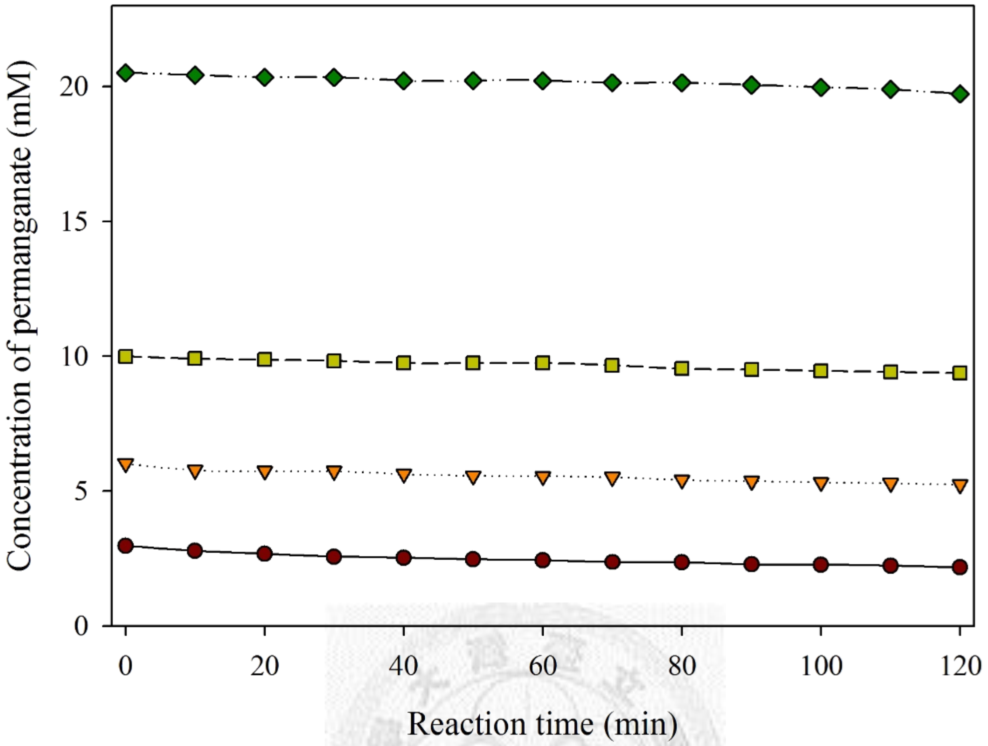

Fig. 4-4 Time dependent variation of permanganate concentration in PM-US system with initial pH=4 and ultrasonic irradiation (60μm, 150W, 40kHz) at 30℃.

Table 4-1 Analysis results of element composition of precipitate in permanganate-ultrasonic system by Energy Dispersive Spectrometer

Element	Weight%	Atomic%
Oxygen	38.39	68.15
Manganese	61.61	31.85
Total	100	

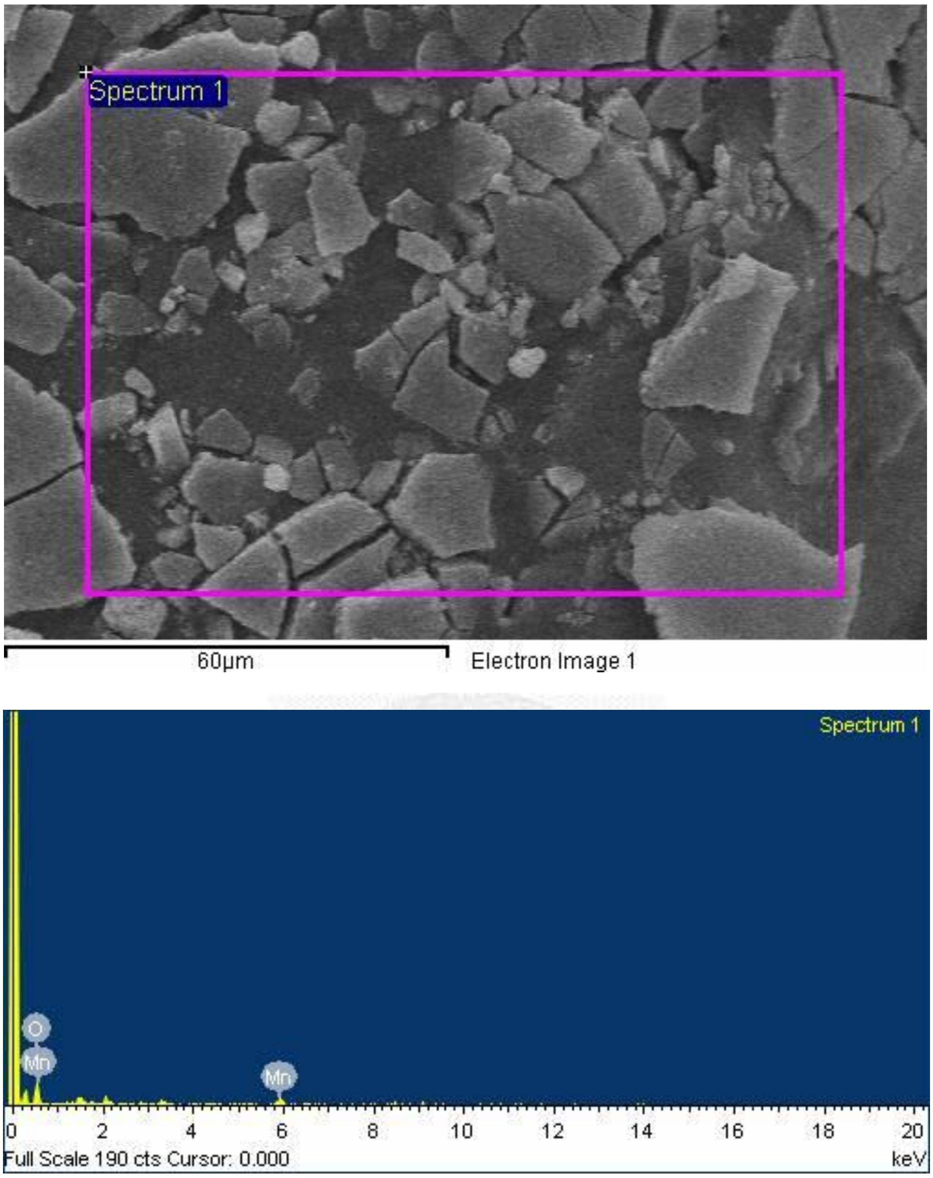

Fig. 4-5 Physicochemical analysis results carried out by Scanning Electron Microscope and Energy Dispersive Spectrometer.

4.3 Effects of amplitude of ultrasonic waves on PFOA decomposition

Amplitude of ultrasonic waves is a major operating parameter. In a study about influenced factors on output power by ultrasound (Raso et al., 1999), at all pressures tried, power output increased exponentially when the amplitude was increased. But the influenced way of amplitude in PFOA degradation process was still unknown. The effect of amplitude on PFOA decomposition was carried out in Fig.4-6. Decomposition efficiency of PFOA increased from 24.7% to 82.4% as the amplitude raised from 20μm to 60μm.

Rate constant of PFOA decomposition increased linearly in the amplitude range (Fig.4-7). However, the rate constants of defluorination did not improve as decomposition from amplitude of 40μm to 60μm. $K_{1\mathrm{bos}}$ at amplitude of 60μm is 1.9 times relative to that at 40μm, while $K_{2\mathrm{obs}}$ was only 1.1 times. Amplitude effect in ultrasonication due to the increased size of reactive volume (Wu et al., 2006) and range of bubble sizes (Suslick, 1990) undergoing cavitation at higher amplitude. And cavitation was reported as a dominant impact in ultrasonication for pyrolytic reactions and cleavage steps (decomposition) that prior to fluoride production (defluorination) (Vecitis et al., 2008). Therefore, limited increment of defluorination rate by raised amplitude of ultrasonic waves may indicate that amplitude mainly influence the decomposition part in PFOA degradation process.

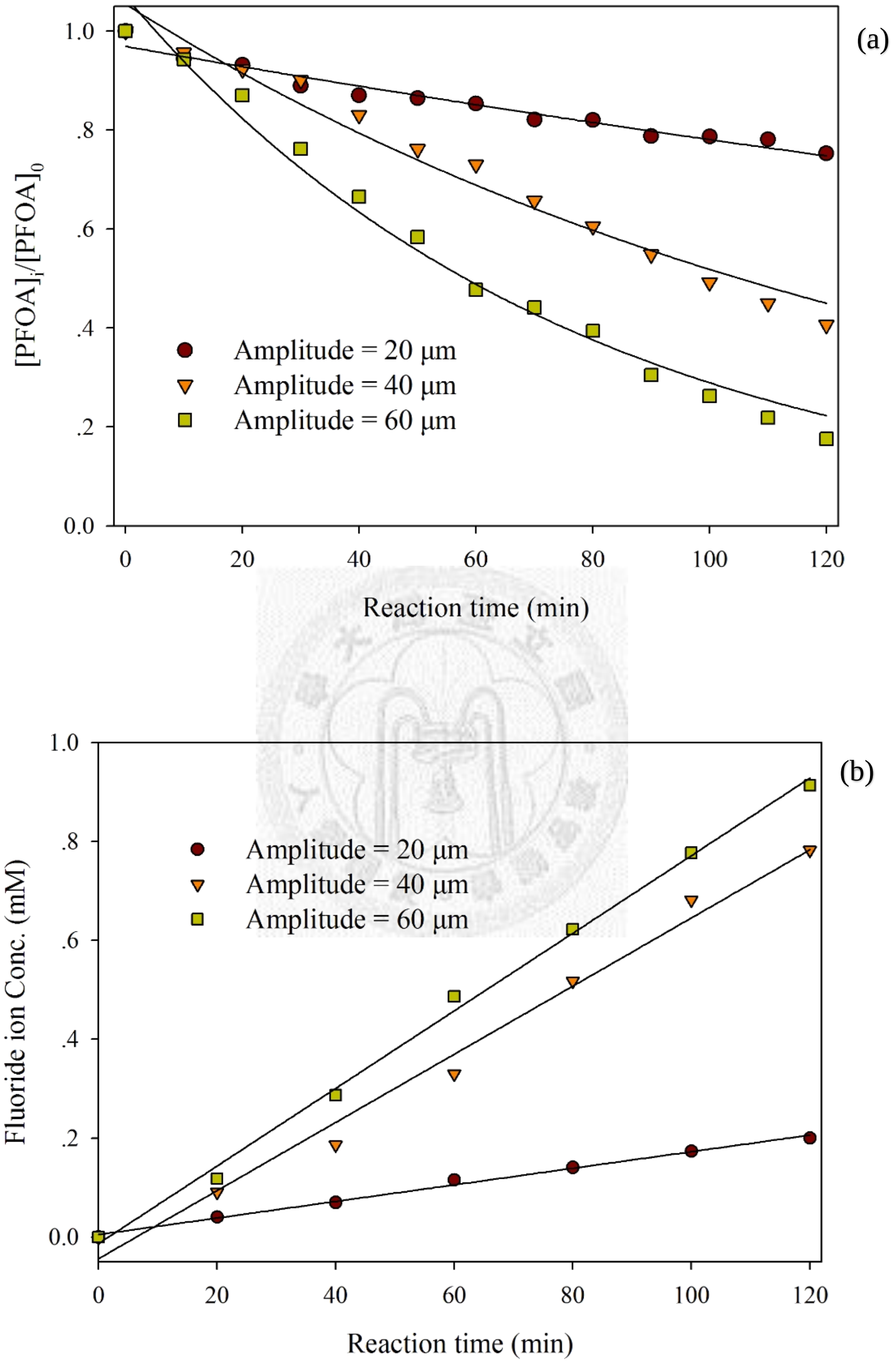

Fig. 4-6 Effects of amplitude (20, 40 and 60μm) of ultrasonic waves on PFOA (132 μM) decomposition (a) and defluorination (b) with 6 mM $KMnO_4$ in ultrasonic system (150W, 40kHz) at 30℃, initial solution pH=4.

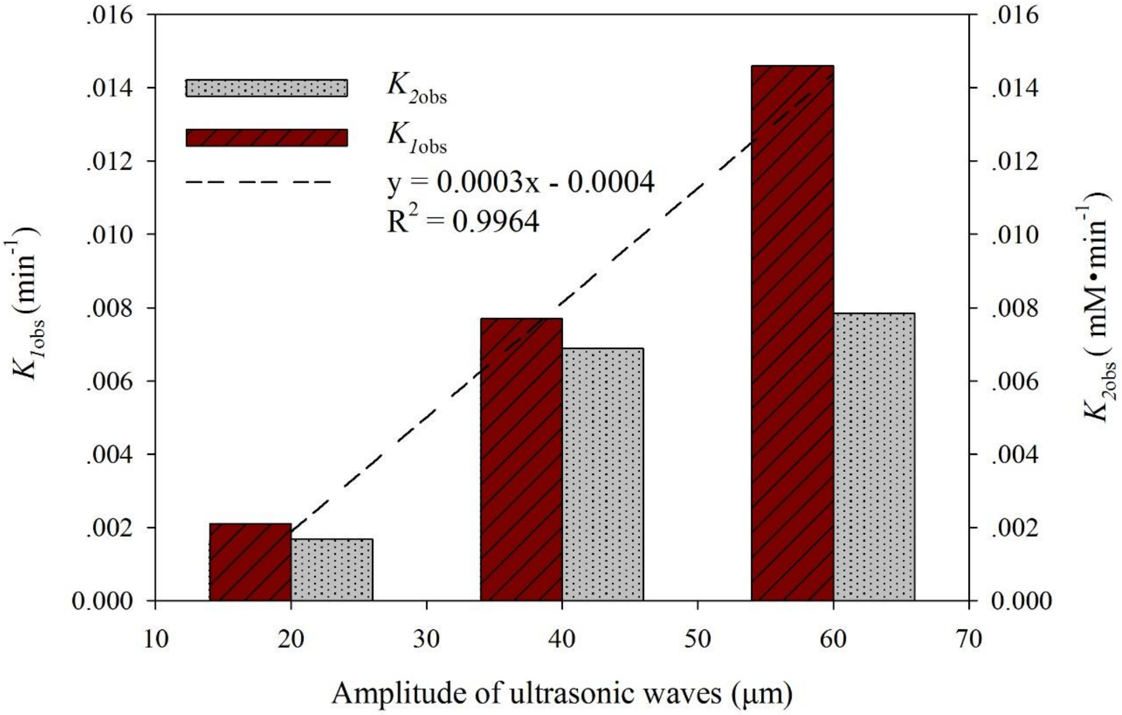

Fig. 4-7 Comparison on kinetics of PFOA (132 μM) decomposition (K_{1obs}) and defluorination (K_{2obs}) with different amplitudes (20, 40 and 60μm) and 6 mM $KMnO_4$ in ultrasonic system (150W, 40kHz) at 30℃, initial solution pH=4.

4.4 Effects of permanganate dosages on PFOA degradation

Comparative degradation of PFOA between varied concentrations of $KMnO_4$ (0, 1, 3, 6, 10, and 20 mM) was carried out. As degradation plots and rate constants of decomposition and defluorination presented in Fig. 4-8 and Fig.4-9, respectively, degradation efficiency and kinetics showed the same tendencies with raised permanganate dosages. The rate of PFOA decomposition increased rapidly with permanganate dosage from 1 mM to 3 mM, but the increment diminished after 3 mM $KMnO_4$. K_{1obs} increased to 3.85 times with adding only 3 mM permanganate, but only increased to 1.25 times from dosage of 3 mM to 20 mM.

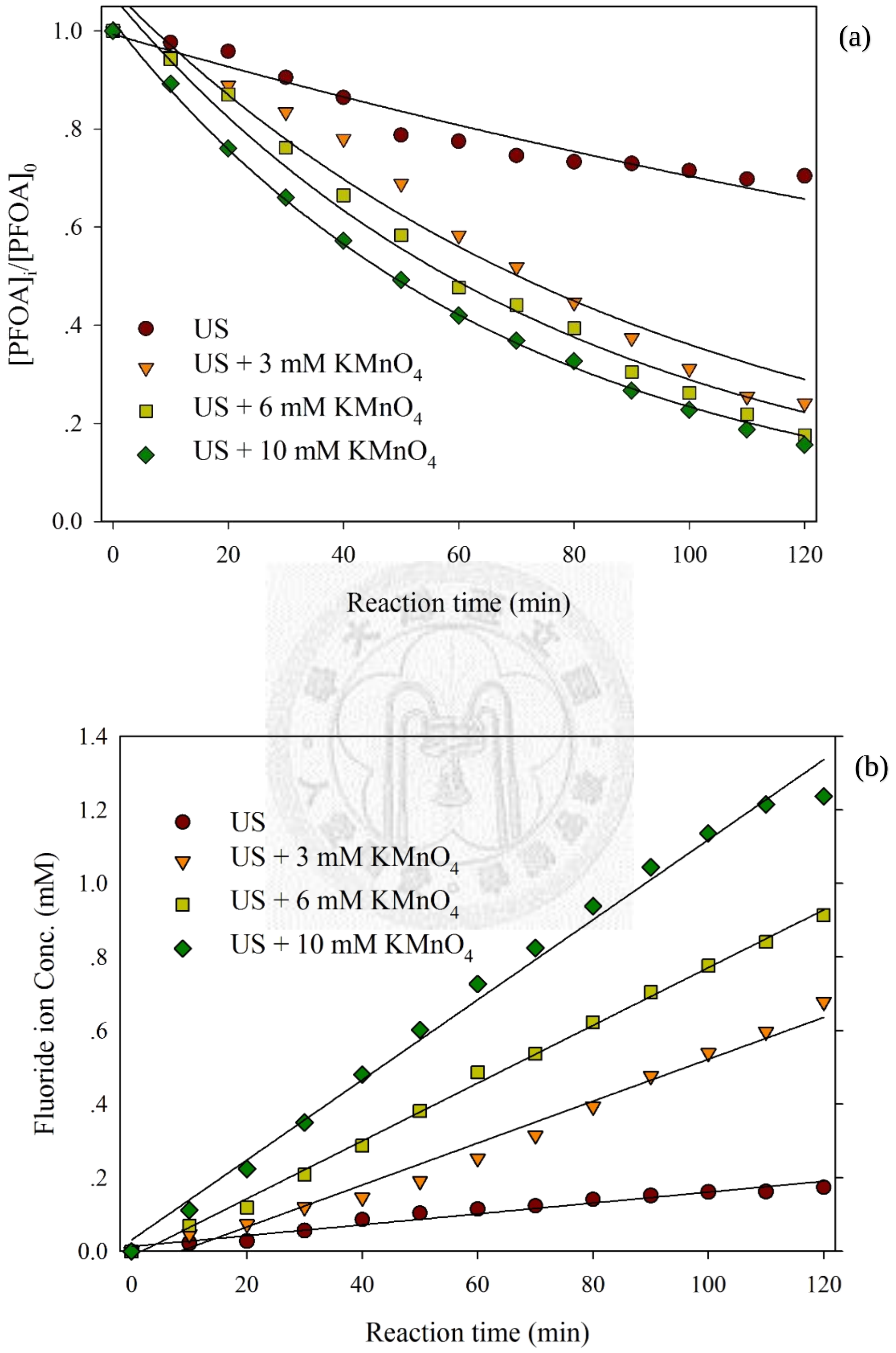

Fig. 4-8 Effects of $KMnO_4$ dosages on PFOA (132 μM) decomposition (a) and defluorination (b) with initial solution pH=4 in ultrasonic system (60μm) at 30℃.

This phenomenon implied that permanganate act as an activator or catalyst in PFOA decomposition reaction under ultrasonic irradiation (Eq. (4-3)). And the activated or catalytic effect stabilize for 132μM PFOA when permanganate dosages over 3 mM.

$$CF_3[CF_2]_6COO^- +))) \xrightarrow{KMnO_4} CF_3[CF_2]_6\cdot + CO_2 \qquad (4\text{-}3)$$

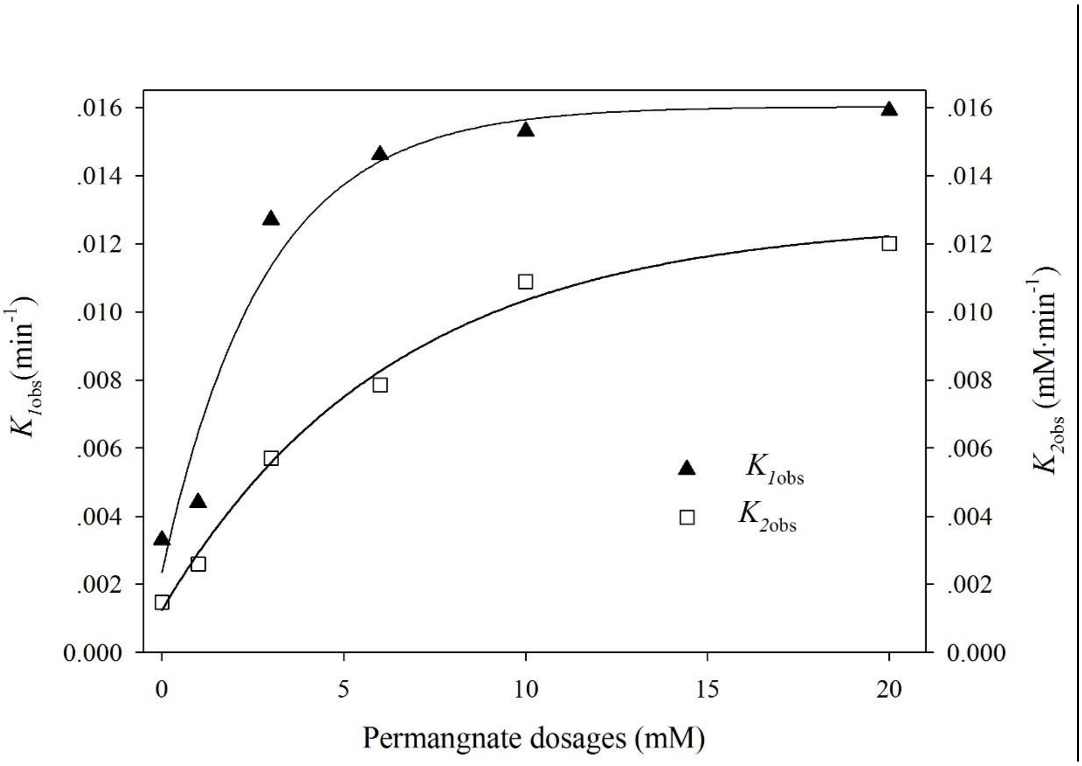

Fig. 4-9 Variation of rate constants of PFOA (132 μM) decomposition (K_{1obs}) and defluorination (K_{2obs}) as a function of $KMnO_4$ dosages (0, 1, 3, 6, 10, 20 mM) under ultrasonic irradiation (60μm, 150W, 40kHz) with initial solution pH=4 at 30℃.

K_{2obs} increased apparently to 7.35 times from permanganate dosages of 0 mM to 10 mM, but increased slightly to 1.10 times from 10 mM to 20 mM. This results might due to the reaction with Mn(II) intermediate to form Mn(III)/Mn(IV), when $KMnO_4$ was overdosed (Han et al., 2013).

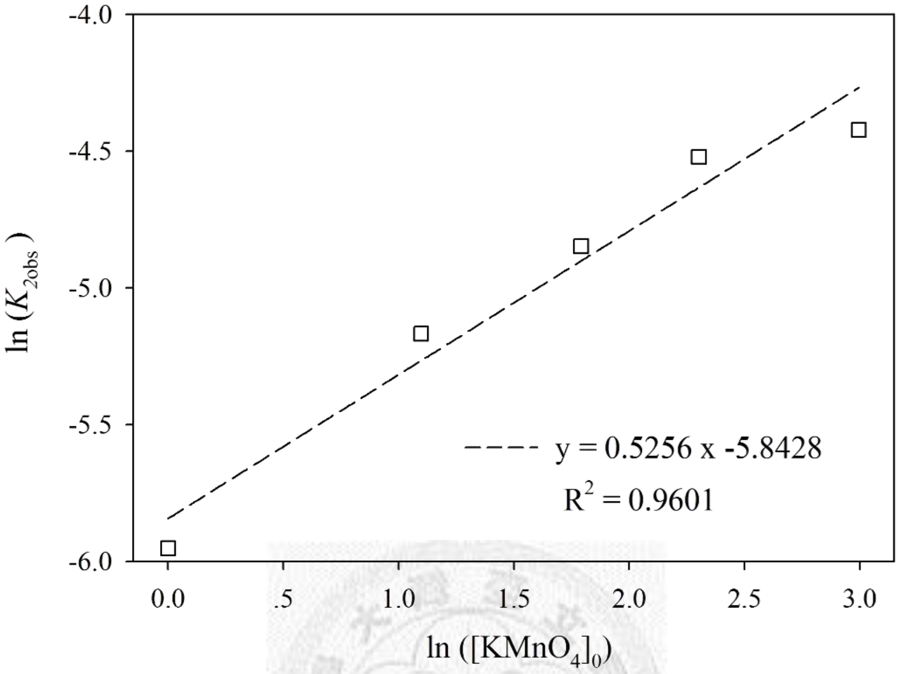

Fig. 4-10 Regression curve of ln(K_{2obs}) versus ln([KMnO$_4$]$_0$) in the dosages range between 0 and 20 mM under ultrasonic irradiation (60μm, 150W, 40kHz) with initial solution pH=4 at 30℃.

However, A plot of ln(K_{2obs}) vs. ln([KMnO$_4$]$_0$) would yield a linear curve (Eq.(4-4)) in the dosages range between 0 and 20 mM with R^2 = 0.96 (Fig. 4-10), and give slop as the stoichiometric number n in defluorination reaction (Eq. (4-5)) where permanganate acted as an oxidant.

$$\ln(K_{2obs}) = n\ln([KMnO_4]_0) + \ln(K_{2obs}{}^0) \qquad (4\text{-}4)$$

$$R\text{-}CF_2\cdot + nMnO_4^- \rightarrow MnO_2 + R\text{-}COO\cdot + 2F^- \qquad (4\text{-}5)$$

Where $[KMnO_4]_0$ is the permanganate dosage, K_{2obs}^0 is K_{2obs} of $[KMnO_4]_0 = 1mM$, $R\text{-}CF_2\cdot$ is perfluoroalkyl radicals. In view of treatment cost and efficiency, permanganate dosages of 3 mM and 10 mM were the optimal dosage for decomposition and defluorination efficiency, respectively.

4.5 Effects of initial solution pH on PFOA degradation

The variation of solution pH was widely reported to influence oxidation performance of $KMnO_4$ (Damm et al., 2002; Aleboyeh et al., 2009; Han et al., 2013) and PFOA degradation (Sri Chandana Panchangam, 2009). The effects of initial solution pH on PFOA decomposition are presented in Fig.4-11.

PFOA decomposed more effectively under acidic (pH=4, 84.3%) and highly alkaline (pH=11, 76.8%) condition than that under highly acidic (pH=2, 59.8%) and neutral (pH=7, 32.4%) condition. Plotting rate constant of PFOA decomposition and defluorination, respectively, vs. pH in the range of 2 to 11, K_{1obs} and K_{2obs} reach their peak at pH=4.

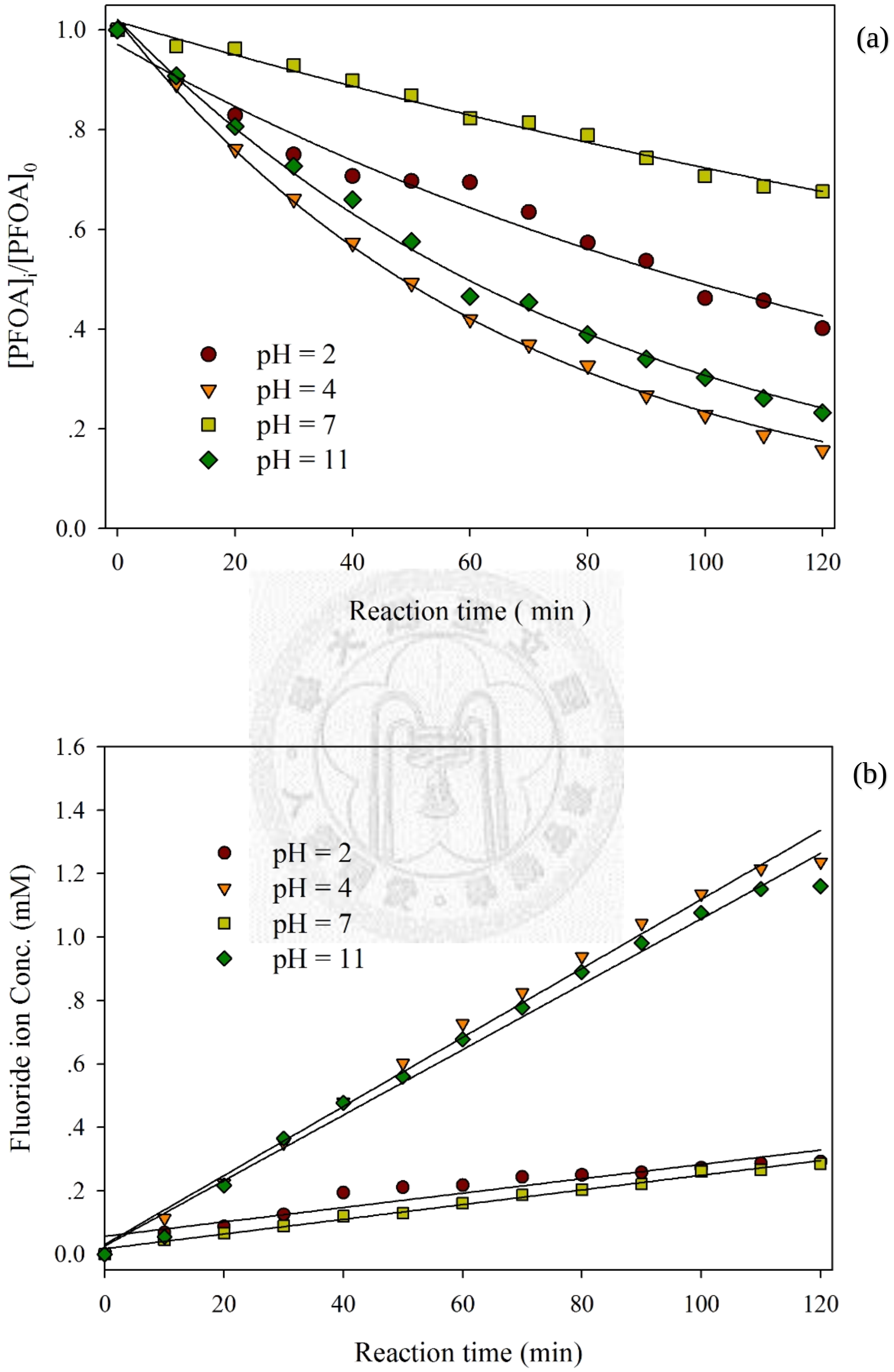

Fig. 4-11 Effects of initial solution pH on PFOA (132 μM) decomposition (a) and defluorination (b) with 10 mM $KMnO_4$ in ultrasonic system (60μm, 150W, 40kHz) at 30 ℃.

According to the stoichiometric equations shown in section 2.2 (Eqs. (2-3)-(2-7)) (Yan and Schwartz, 1999), $[H^+]$ determines the reactivity of permanganate resulting in different redox pathways and redox potential (Pe^0) of permanganate increase with pH decline. Under highly acidic condition (pH<3.5), one permanganate undergoes a five-electron exchange (Eq.(2-3)) with $Pe^0 = +25.5$. From pH=3.5 to 12, one permanganate undergoes a three-electron exchange via Eq. (2-4) in acidic pH conditions and Eq. (2-5) in neutral or alkaline condition completed with $Pe^0 = +28.7$ and +9.9, respectively. Under highly alkaline (pH>12) condition (Eq. (2-6)), one-electron exchange take place and Pe^0 is only +9.5. MnO_2, as the reduction products, also own oxidation capacity under acidic condition with a considerable $Pe^0 = 20.8$ (Morel and Hering, 1993) via Eq. (2-7).

Therefore, acidic condition is more stimulative than neutral condition for oxidation by permanganate, and it should be expected that higher PFOA degradation efficiency would be observed at lower pH than 4. However, $K_{1\mathrm{obs}}$ and $K_{2\mathrm{obs}}$ with initial pH=3 and 2 presented in Fig. 4-12, deviated from this expection, decline remarkably.

$K_{1\mathrm{obs}}$ with initial pH=3 and 2 are 0.93 and 0.46 time as compare to that with initial pH=4, $K_{2\mathrm{obs}}$ of initial pH=3 and 2 are 0.53 and 0.21 time relative to that with initial pH=4. This phenomenon due to the molecular form and vapor pressure of PFOA switched in a certain level as pH changed.

$$pK_a = -0.1278\,[\mathrm{PFOA}] + 3.8437 \qquad (4\text{-}6)$$

When [PFOA] = 132 μM in this study, the pK_a of PFOA in solution is 3.8 ± 0.1 (Eq. (4-6)).

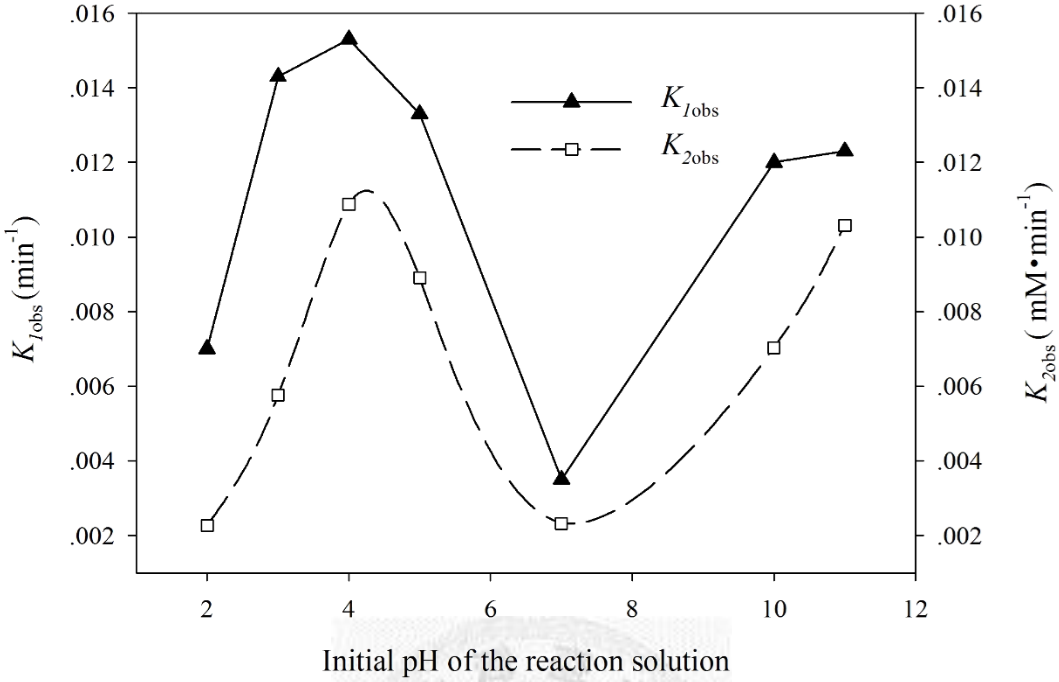

Fig. 4-12 Variation of rate constants of PFOA (132 μM) decomposition ($K_{1\mathrm{obs}}$) and defluorination ($K_{2\mathrm{obs}}$) as a function of initial solution pH (2, 3, 4, 5, 7, 10, 11) with 10mM $KMnO_4$, under ultrasonic irradiation (60μm, 150W, 40kHz) at 30℃.

Accordingly, anionic form ($C_7F_{15}COO^-$) will transform gradually to neutral form ($C_7F_{15}COOH$) from under acidic (pH > 3.8) to highly acidic (pH < 3.8) condition. As discussed by Burns, within the highly acidic solution, especially where pH≈2, almost 99% of the total PFOA will be presented as the neutral acid species ($C_7F_{15}COOH$). And vapor pressure of PFOA would vary as its molecular transform. According to the results presented in a study about Henry's law constant (K_H) of PFOA at 298 K in aqueous sulfuric acid solutions (Kutsuna and Hori, 2008), the K_H ($\mathrm{mol{\cdot}dm^{-3}{\cdot}atm^{-1}}$) of PFOA would augment with increased H_2SO_4 dosages followed by PFO transform to PFOA. Therefore, although the pK_a value of PFOA is low, the relatively lower solution pH (ex. initial pH=2) favor partitioning of PFOA into the gas phase (Armitage et al., 2009). Ultrasonic degradation is effective for the removal of contaminants with high Henry's Law constants that partition into the vapor phase of the bubble or for surfactants, such as PFOA, that partition to the air-water interface (Vecitis et al., 2008). Average temperature raise to 4000 K in internal vapor phase and 600-1000 K on bubble-water interface via transient collapse of aqueous cavitation bubbles under ultrasonication. Under $pH < 3.8$ condition, PFOA partition into the vapor phase, which might promote PFOA decomposition under the higher pressure and temperature condition but also lead to the absence of activation by permanganate. The results showed in Fig. 4-12 demonstrated that overall the activation by permanganate is more significant than the high pressure and temperature condition, and highly acidic condition is disadvantageous for PFOA degradation in ultrasonic system. $K_{2\mathrm{obs}}$ declined more than $K_{1\mathrm{obs}}$ also correspond to the fact that partioning into bubbles impact PFOA defluorination process more than decomposition process. At pH = 4, which is greater than $pK_a = 3.8 \pm 0.1$, PFO is dominated species. So initial solution pH = 4 was adopted as optimal pH for both decomposition of PFOA and oxidation by permanganate.

Degradation performance of PFOA under highly alkaline condition (pH>10) were not as poor as the oxidation by permanganate ($Pe^0 = +9.9$). $K_{1\mathrm{obs}}$ with initial pH=10 and 11 were 3.43 and 3.51 times of that with initial pH=7, $K_{2\mathrm{obs}}$ were 3.03 and 4.44 times, respectively. According to these variation we considered the PFOA degradation rate increase gradually with the increased pH when pH>7. Similar enhancement (1.18 times) in decomposition rate constants is observed when adjusting pH from 8 to 11 in the investigation of sonochemical degradation of PFOA in groundwater (Cheng et al., 2009). This might be interpreted by that higher OH^- concentration in alkaline condition would produce more $OH\cdot$ radicals which could act as activator as permangante. The diminished increment from pH=10 to 11 in decomposition rate and linear enhancement from pH=7 to 11 in defluorination (Fig. 4-12) also corresponding well to the effect of permanganate dosages (Fig. 4-9). Tert-butyl alcohol (TBA), as a radicals scavenger, was add to PM-US system in alkaline condition to prove the activated effect of OH· radicals. The comparison on decomposition rate was presented in Fig. 4-13.

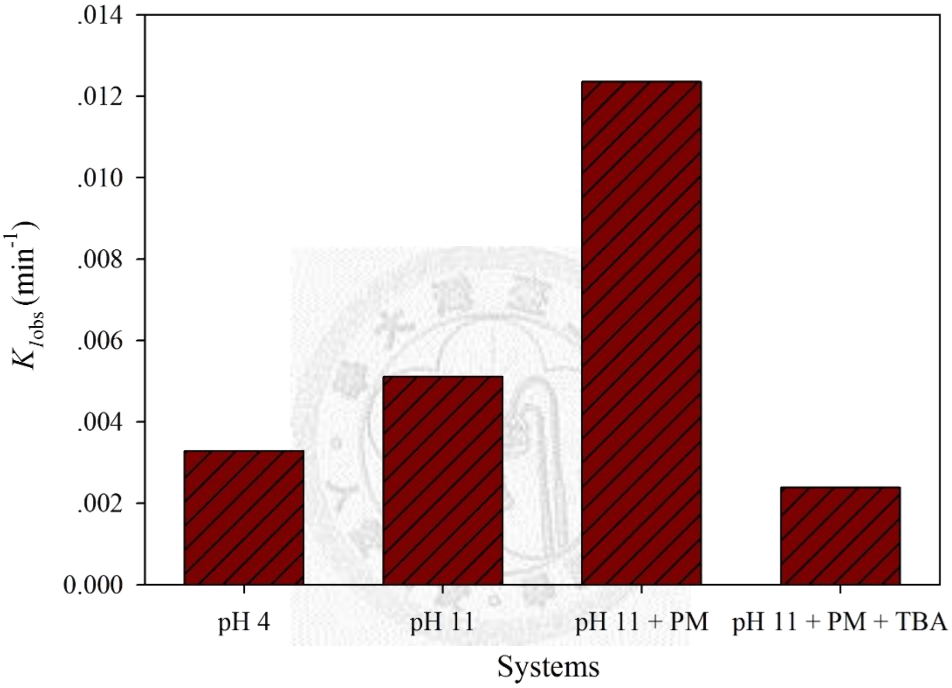

Fig. 4-13 Comparison on kinetics of PFOA (132 μM) decomposition (K_{1obs}) under different conditions (pH=4, pH=11, 10 mM $KMnO_4$ at pH=11, and 10 mM $KMnO_4$+10 mM tert-butyl alcohol (TBA) at pH=11) in ultrasonic system (60μm, 150W, 40kHz) at 30℃.

Without permanganate, PFOA decomposed more effective with initial pH=11 than 4 for more activation by OH· radicals at alkaline condition; adding 10mM $KMnO_4$ to alkalization solution, K_{1obs} increase again for synergistic effect of permanganate and OH·

radicals; adding 10mM TBA to PM-US system with initial pH=11, $K_{1\mathrm{obs}}$ decrease remarkablly and even lesser than $K_{1\mathrm{obs}}$ of mono-US system with initial pH=4. This Comprative result indicate OH· radicals is a significant activator, assisted by permanganate, under alkaline condition in PM-US system for PFOA decomposition. Solution pH under alkaline condition decline with reaction time (Fig. 4-14) also witnessed the OH^- consumption during ultrasonication. Although TBA also would scavenge perfluoroalkyl radicals that are products of PFOA decomposition, TBA would not restrict PFOA decomposition rate. And the influences of permanganate consumption via TBA oxidation were ignorable as the relatively abundant amount of permangante.

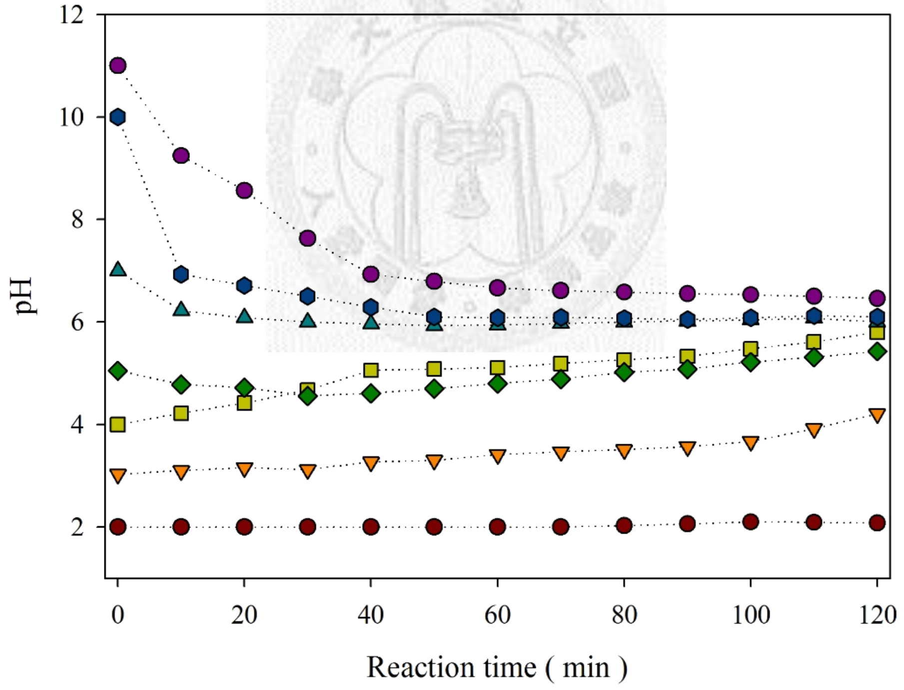

Fig. 4-14 Solutions pH varied with reaction time in permanganate-ultrasonic system ($[PFOA]_0$=132μM, $[KMnO_4]_0$=10mM, under ultrasonic irradiation (60μm, 150W, 40kHz) at 30℃).

With 132μM PFOA and varied initial pH, solution verge to weak acidic condition in PM-US system (Fig.4-14). It is verified above that hydroxyl radicals would be consumed under ultrasonic irradiation. So pH of basic and neutral solution would decrease with time. Decomposition of PFOA, as a weak acid, would increase solution pH. In weak acidic solution (pH=5), pH decreased in the first half hour and increased in the rest of time was the result of hydroxyl radicals consumption and PFOA decomposition. In acidic solution (pH=3 and 4), pH increased throughout as hydroxyl radicals consumption was negligible. And PFOA decomposition was negligible on pH change when reaction was under highly acidic condition (pH=2).

4.6 Effects of solution temperature on PFOA degradation

Although power output of ultrasonication decreased as the temperature was raised at constant amplitude and pressure (Raso et al., 1999), higher temperature would activate the oxidation reaction by permanganate (Liu et al., 2009). Temperature effect on PFOA degradation in PM-US system was investigated from 30 to 50℃. As presented in Fig. 4-15, raised temperature increased the rate of PFOA decomposition and defluorination slightly. In the temperature range studied (Fig.4-16), $K_{1\mathrm{obs}}$ and $K_{2\mathrm{obs}}$ follow the Arrhenius law (Eq. 4-7) applied widely in investigations of sonochemical degradation (Suslick et al., 1983; Goskonda et al., 2002) and oxidation with permangante (Liu et al., 2009).

$$\mathrm{K_{obs}} = \mathrm{A}\ \exp\left(\frac{-\mathrm{E_{a\,obs}}}{\mathrm{RT}}\right) \qquad (4\text{-}7)$$

Where $\mathrm{K_{obs}}$ is the rate constant of PFOA decomposition or defluorination, A is pre-exponential factor in unit identical to K_{obs}, $\mathrm{E_{aobs}}$ is apparent activation energy for PFOA decomposition ($\mathrm{E_{a1obs}}$) or defluorination ($\mathrm{E_{a2obs}}$), R is the Universal gas constant, T is the liquid temperature in kelvin.

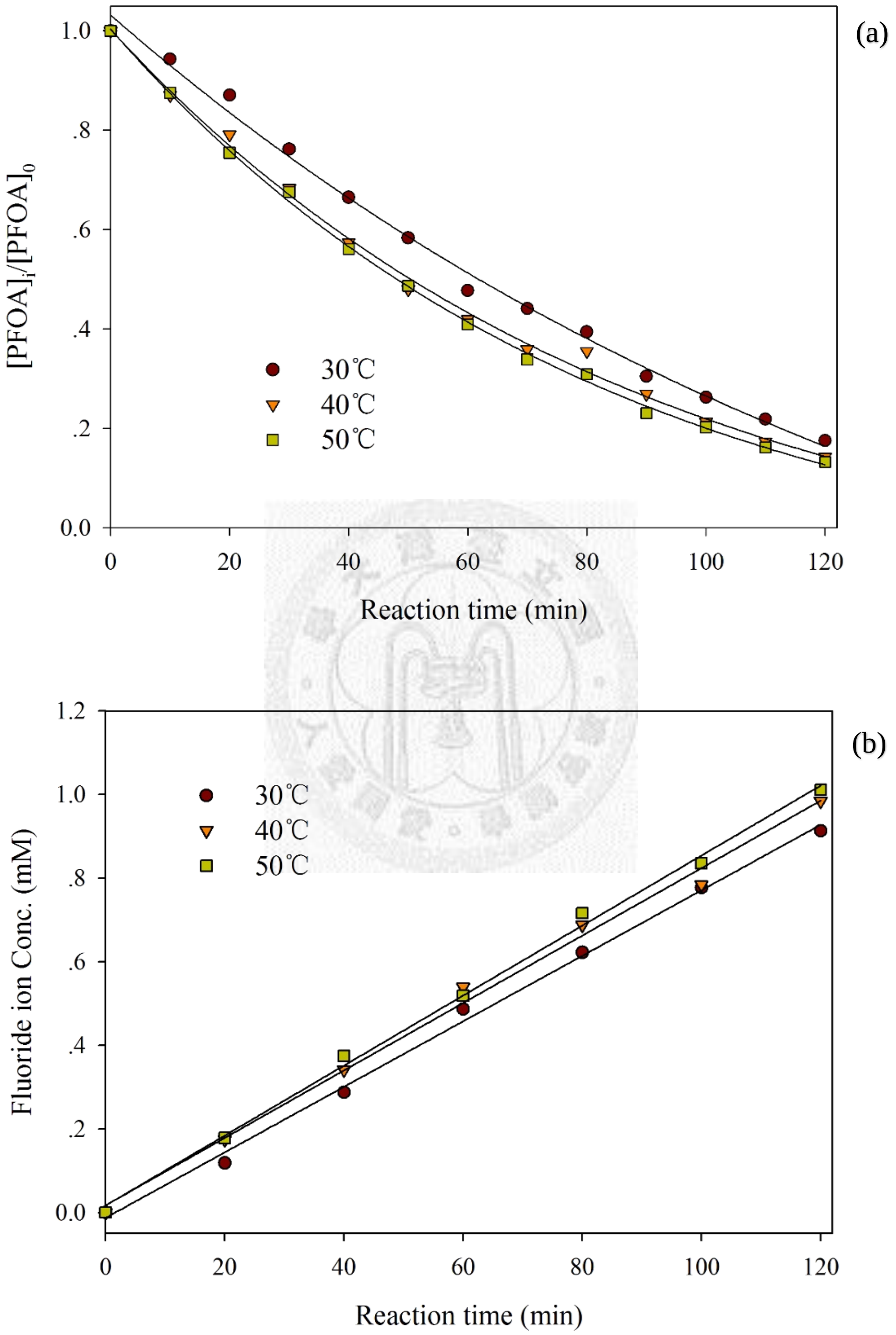

Fig. 4-15 Effects of solution temperature on PFOA (132 μM) decomposition (a) and defluorination (b) with 6mM $KMnO_4$ and initial solution pH=4 under ultrasonic irradiation (60μm, 150W, 40 kHz).

E_{a1obs} and E_{a2obs} are carried out to be +5.734 $kJ \cdot mol^{-1}$ and +2.655$kJ \cdot mol^{-1}$, respectively. Increased temperature seemed to accelerate PFOA degradation rate in PM-US system. But E_{a1obs} and E_{a2obs} are far small than reported activation energy of the oxidation by permanganate for dichlorvos (+25.9 $kJ \cdot mol^{-1}$) and microcystins (+28.8 $kJ \cdot mol^{-1}$) (Liu et al., 2009). This phenomenon due to the opposite effect of increased temperature on oxidation by permanganate and ultrasonic system, respectively.

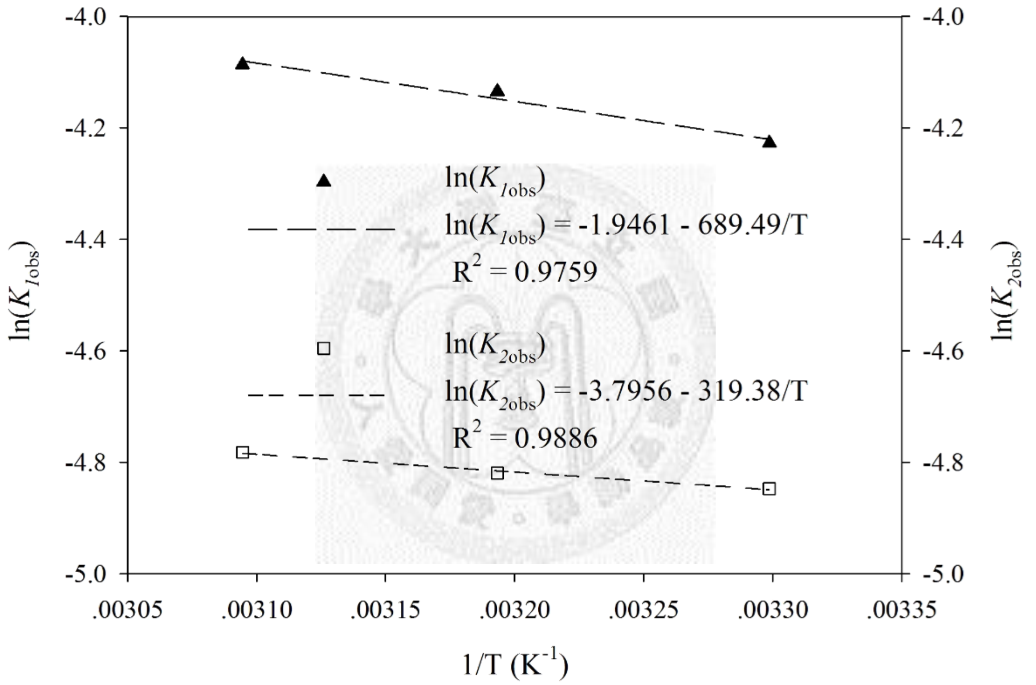

Fig. 4-16 Arrhenius plot of PFOA decomposition (K_{1obs}) and defluorination (K_{2obs}) at from 30℃ to 50℃ in PM-US system with 6mM $KMnO_4$ and initial pH=4, under ultrasonic irradiation (60μm, 150W, 40 kHz).

The majority of mechanical process, including sonochemical degradations, are decelerated by an increase in temperature (Price and Smith, 1993). Decrease in rate constant of sonochemical degradation with higher temperature had been noted by researchers (Goskonda et al., 2002; Jiang et al., 2006). This negative effect of temperature could be interpreted by that higher temperature would result in: (1) decreased viscosity of solvent (water) that leads to worse transmission of the ultrasound through the liquid (Malhotra, 1986); (2) and increased vapor pressure of solvent that leads to disabled cavitation bubbles after coalescence (Jiang et al., 2006) and lessened shock waves (Price and Smith, 1993). So the temperature effect of sonochemical degradation was taken into consider and derived Arrhenius law for ultrasonication formed (Eq. (4-8)) (Suslick et al., 1983):

$$\ln(\mathrm{K}) = \ln\mathrm{A} - \frac{\mathrm{E_a}}{\mathrm{RTP}_a(\Upsilon-1)}\mathrm{P}_\upsilon = \ln\mathrm{A} - \frac{\mathrm{E_{aUS}}}{\mathrm{RT}} \tag{4-8}$$

Where E_a is a positive constant independent with temperature T; P_a is acoustic pressure at initiation of collapse; P_υ is the vapor pressure of water at temperature T and a function of T (Antoine equation); Υ is the ratio of specific heat; E_{aUS}, as a negative apparent constant (Price and Smith, 1993), decrease with raised temperature. On the other hand, oxidation by permanganate follow strictly the original Arrhenius law (Eq. (4-9)),

$$\ln(\mathrm{K}) = \ln\mathrm{A} - \frac{\mathrm{E_{aPM}}}{\mathrm{RT}} \tag{4-9}$$

$$\ln(\mathrm{K_{obs}}) = \ln\mathrm{A} - \left(\frac{\mathrm{E_{aUS}}}{\mathrm{RT}} + \frac{\mathrm{E_{aPM}}}{\mathrm{RT}}\right) = \ln\mathrm{A} - \frac{\mathrm{E_{aobs}}}{\mathrm{RT}} \tag{4-10}$$

E_{aPM} is a positive apparent constant. All activation energy E_a dependent on specific reaction and medium. Therefore, when E_{aUS} decrease considerably with increased temperature to lead $E_{aobs} < 0$ (Eq. (4-10)), PFOA degradation in PM-US system would slow down. Clearly, optimal reaction temperature for decomposition and defluorination, respectively, in PM-US system were existed and the temperature rang in this study has not cover the optimun yet.

4.7 Effects of co-dissolved heavy metal cations on complexes formation and PFOA decomposition

The impact of heavy metal cations on PFOA degradation was investigated using Cu^{2+}, Fe^{2+} and Fe^{3+} with dosages of 0.2 mM. The comparison results of decomposition and defluorination rate were presented in Fig.4-17 and Fig.4-18. It can be seen in Fig.4-17(a) that the concentration of PFOA unstable during ultrasonication in the presence of Fe^{3+}. PFOA might form complexes with Fe^{3+} resulting in rapidly declined concentration of free PFOA anions. And PFOA anions would regain for the PFOA-Fe^{3+} complexes dissolved into water (Fig.4-17(a)). For this phenomenon, quantification of PFOA concentration and rate constants of PFOA decomposition might be unpersuasive due to the influence of heavy metal cations on PFOA quantification. So defluorination plots and kinetics were used to proof the effects of various heavy metal cations on PFOA degradation. Decrease were observed in both decomposition and defluorination with all heavy metal cations. Similarly decelerated effect was observed in sonochemical-Fenton combined system (Joseph et al., 1999) above 0.1 mM dosage of ferrous ions for azo dyes decolonization. However, effect of metal cations on PFOA degradation had been reported to be improved by Fe^{3+}, Fe^{2+} under ultraviolet irradiation (Wang et al., 2008) and ignorable by Na^{2+}, Ca^{2+}, Mg^{2+} under ultrasonic irradiation.

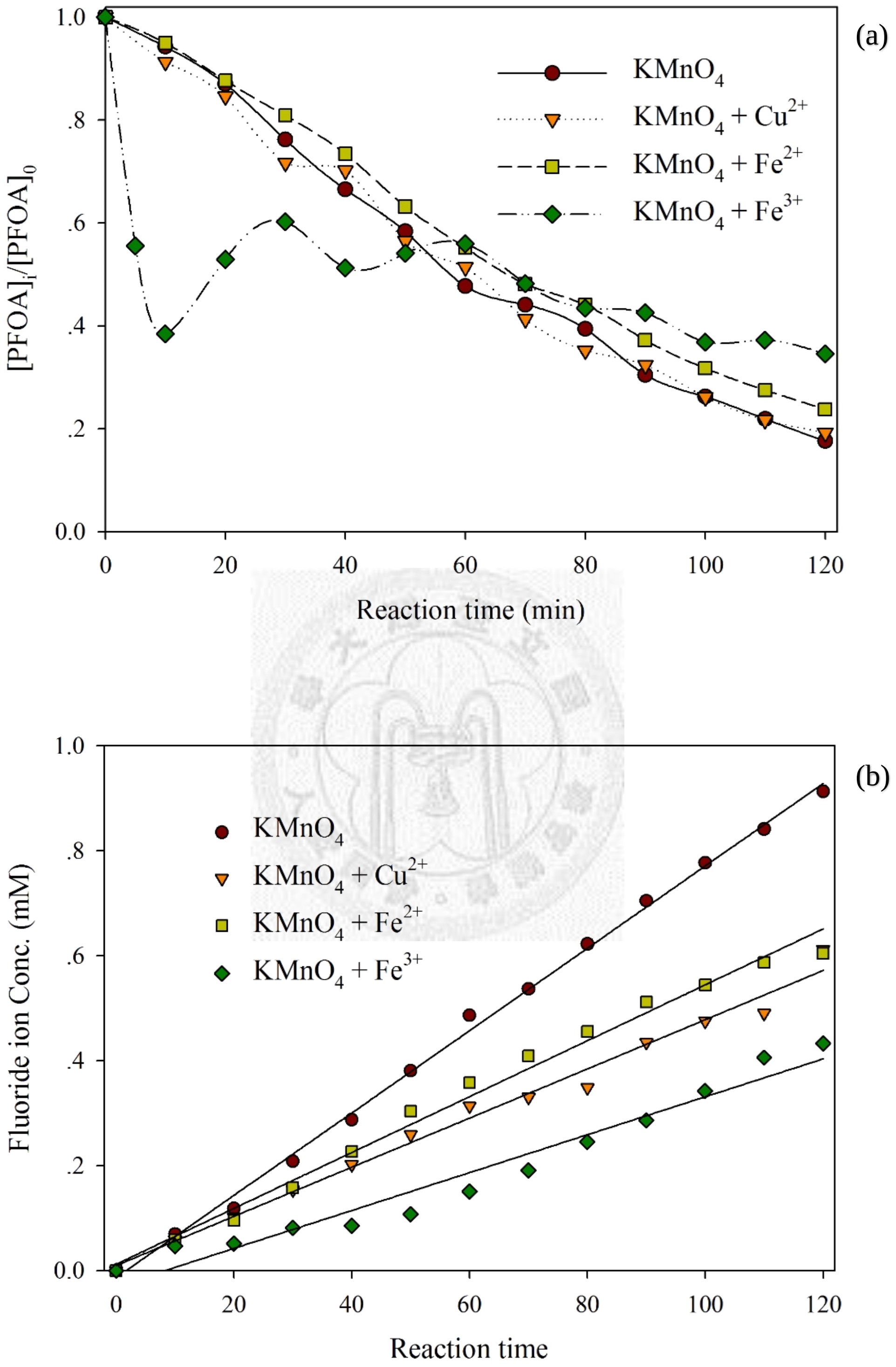

Fig. 4-17 The plots of PFOA decomposition (a) and defluorination (b) with none heavy metal cation, 0.2 mM Cu^{2+}, 0.2 mM Fe^{2+} and 0.2 mM Fe^{3+}, respectively, under ultrasonic irradiation (60µm) with 10 mM $KMnO_4$ and initial solution pH=4 at 30℃.

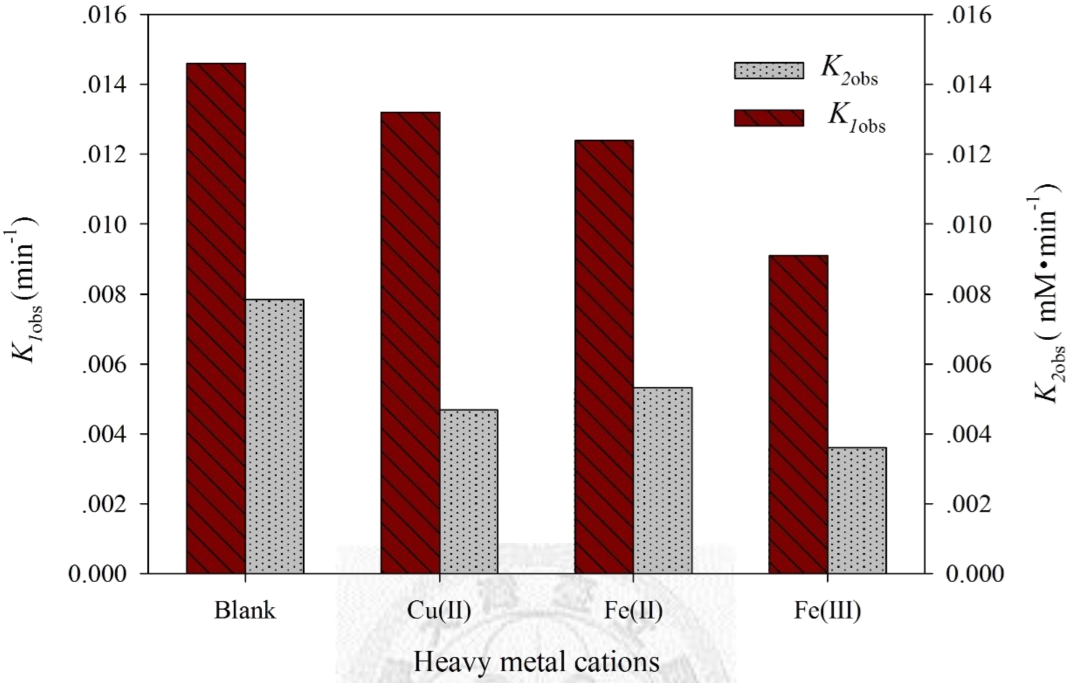

Fig. 4-18 The observed pseudo rate constant of PFOA decomposition (K_{1obs}) and defluorination (K_{2obs}) in the presence of none heavy metal cation, 0.2 mM Cu^{2+}, 0.2 mM Fe^{2+} and 0.2 mM Fe^{3+}, respectively, under ultrasonic irradiation (60µm) with 10 mM $KMnO_4$ and initial solution pH=4 at 30℃

The different effect might be explained by the formation of metal-PFOA complexes. Heavy metal cations, especially ferric ion, are more likely, with high stability constants, to form complexes with carboxylic groups of PFOA than alkaline metals or alkaline earth metals. As presented in Fig.4-19, the concentration of free monomeric PFOA decreased with increased dosages of heavy metal cations. 94.1%, 94.3% and 33.6% of monomeric PFOA remained with 0.2mM Cu^{2+}, Fe^{2+} and Fe^{3+}, respectively, at pH=4. In photochemical system, mixing with heavy metal cations would improve the ultraviolet absorption of

PFOA in a wide region from 200 nm to 400 nm and catalyze the ligand-to-metal charge transfer resulting in photolyzing PFOA to perfluoroalkyl radicals. However, different degradation mechanisms in sonochemical system make heavy metal cations adverse for PFOA degradation. As mentioned above in 3.2, surfactant PFOA would be pyrolyzed, as the decomposition step, on the air-water interface of cavitation bubbles. Coordinated with heavy metal cations, resulting in precipitation in liquid phase, would obviously abate PFOA concentration on the interface regions. In that case, the rate of PFOA decomposition in the presence of Cu^{2+}, Fe^{2+} and Fe^{3+} would decrease in order as the residual concentration of monomeric PFOA decreased, which was depicted in Fig. 4-18. With decomposition of monomeric PFOA, PFOA in complex form would stepwise return to monomeric form.

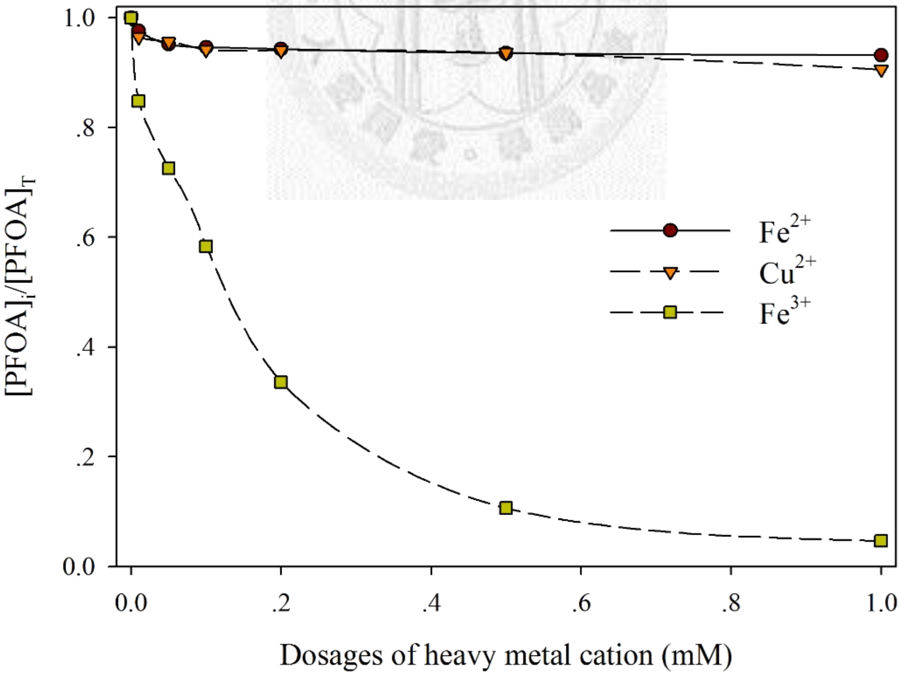

Fig. 4-19 Effects of cation concentration of three heavy metals (Fe^{2+}, Cu^{2+} and Fe^{3+}) on residual concentration of free PFOA at pH=4.

The other factor of effects with heavy metal cations might be the pH changes occurred when adding metal heavy metal cations into solutions. pH of solution with 0.2 mM Fe^{3+} would be suppressed from 4 to roughly 3.3 as the formation of $Fe(OH)_3$ precipitation. The acidification process was approved in section 4.5 to impact PFOA decomposition.

4.8 Effects of atmosphere on PFOA defluorination

In order to investigate the effect of atmosphere on PFOA defluorination, a set of comparative experiments was carried out between permanganate and perhydrol (PH) under argon, air and oxygen atmosphere, respectively. Although the oxidation potential Pe^0 of hydrogen peroxide is 30.0 and greater than that of permanganate (Eq. (2-4)), perhydrol performed far worse than permanganate with same dosages in activation of defluorination and even decelerated the PFOA defluorination reaction (Fig.4-20). With 6mM dosages, K_{2obs} in perhydrol-ultrasonic (PH-US) system is only 0.56 and 0.11 time of that in mono-US and PM-US system, respectively.

The comparative results presented in Fig. 4-21 showed apparent influences of different atmosphere on PFOA defluorination in PM-US and PH-US system. Relatively low rates of PFOA defluorination were observed under oxygen atmosphere as compare to under air and argon atmosphere. In PM-US system, with 6 mM $KMnO_4$, K_{2obs} under oxygen atmosphere is only 0.72 time of that under air atmosphere. On the contrary, K_{2obs} under argon atmosphere is 1.57 times of that under air atmosphere and even greater than K_{2obs} with 20mM $KMnO_4$ under air atmosphere. Similar effect of atmosphere in PH-US system was observed. K_{2obs} under oxygen and argon atmosphere are 0.51 time and 2.40 times relative to that under air atmosphere. Defluorination rate in PFOA Photodegradation was reported to be decelerated considerably as well with increased dissolved oxygen (Giri et al., 2012).

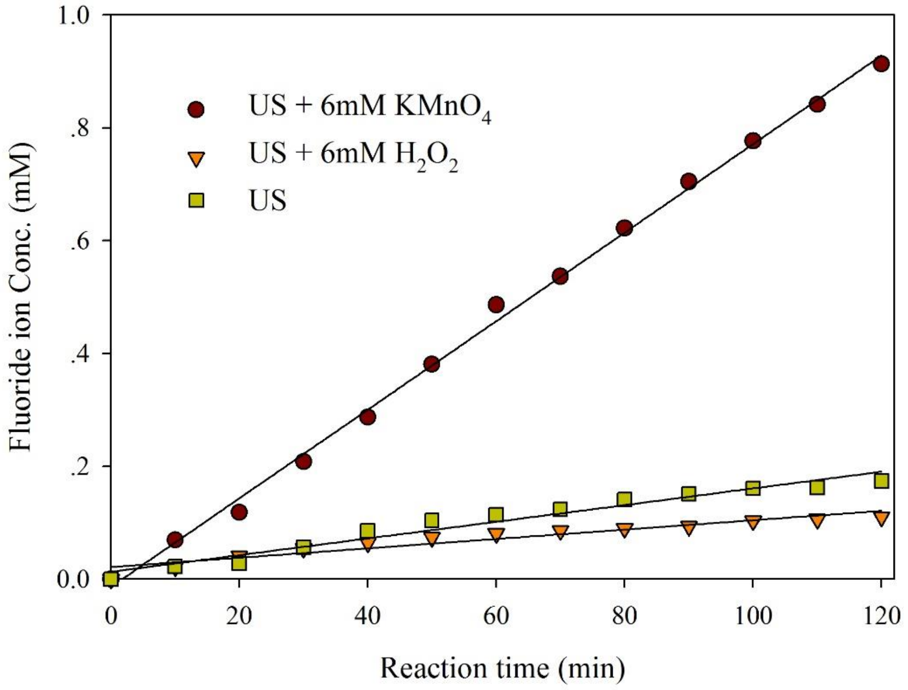

Fig. 4-20 Comparison on PFOA (132 μM) defluorination in PM-US, mono-US and PH-US system, with 6 mM $KMnO_4$ or 6 mM H_2O_2 dosage, under ultrasonic irradiation (60μm, 150W, 40kHz) at 30℃, initial pH=4.

The underlying factor is the adverse effect of oxygen, as an inhibitor or retarder, by terminating the radical's chain reaction. Autoxidation of many hydrocarbons, ethers, aldehydes and unsaturated esters can be described by the representative equation Eq. (4-11)-(4-13).

$$\text{Initiator} \rightarrow R\cdot \quad (4\text{-}11)$$

$$R\cdot + O_2 \rightarrow ROO\cdot \quad (4\text{-}12)$$

$$ROO\cdot + RH \rightarrow ROOH + R\cdot \quad (4\text{-}13)$$

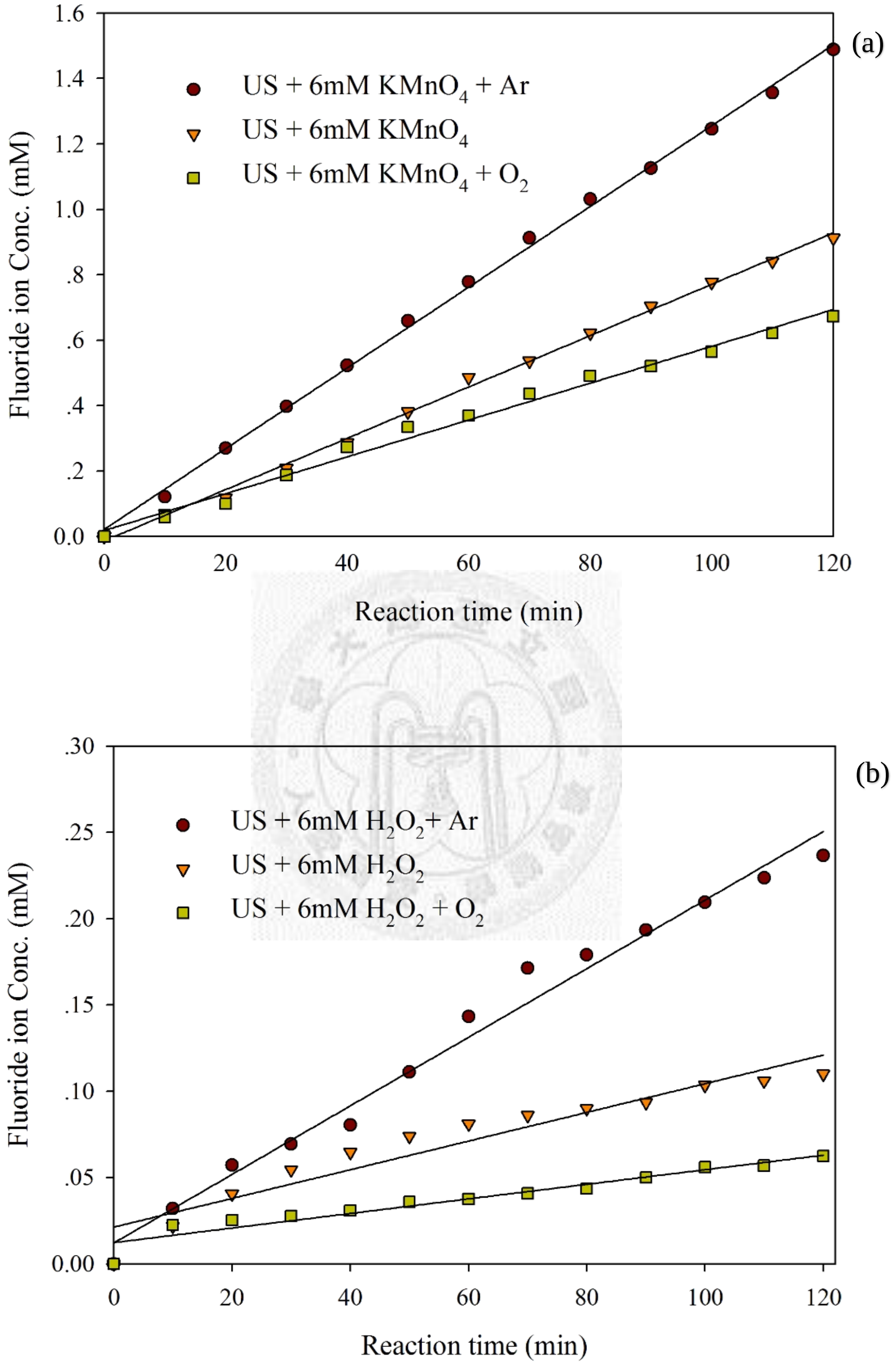

Fig. 4-21 Effects of aeration with argon or oxygen gas on PFOA (132 μM) defluorination with 6 mM $KMnO_4$ (a) or 6 mM H_2O_2 (b) dosage, under ultrasonic irradiation (60μm, 150W, 40kHz) at 30℃, initial pH=4.

And chain termination (Eq. (4-14)-(4-16)) would take place via interaction of any two radicals presented above (Bartlett and Traylor, 1963). The Eq. (4-15), the interaction of two alkylperoxy radicals, is the important chain-terminating step in the region of 1 atm pressure.

$$R\cdot + R\cdot \rightarrow R\text{-}R \tag{4-14}$$

$$ROO\cdot + ROO\cdot \rightarrow ROO\text{-}OOR \tag{4-15}$$

$$ROO\cdot + R\cdot \rightarrow ROOR \tag{4-16}$$

Perfluoro- and fluoro-carbon radicals would occur as the intermediates during PFOA pyrolytic decomposition under ultrasonication (Vecitis et al., 2008). For absence of hydrocarbon (RH) in the reaction solution throughout this study, it is impossible for the alkylperoxy radicals ROO · to undergo the reaction (4-13). Therefore, it is numerous possibilities for perfluoro-carbon radicals reacting with oxygen molecular and forming alkylperoxy radicals followed by termination step. Our experimental results indicated that this termination step indeed slower the defluorination process in the presence of abundant oxygen bubbles. The interference of oxygen on PFOA defluorination can be concluded as Eq.(4-17)-(4-18).

$$R\text{-}CF_2\cdot + O_2 \rightarrow R\text{-}CF_2\text{-}OO\cdot \tag{4-17}$$

$$R'\text{-}CF_2\text{-}OO\cdot + R''\text{-}CF_2\text{-}OO\cdot \rightarrow R'\text{-}CF_2\text{-}OO\text{-}CF_2\text{-}R'' + O_2 \tag{4-18}$$

Reaction with hydroxyl radicals (Bremner et al., 2009) and thermal decomposition (Croiset et al., 1997) of hydrogen peroxide in ultrasonic system would also produce oxygen molecular. Chain reactions of H_2O_2 under ultrasonication were shown below:

$$H_2O_2 +))) \rightarrow 2 \cdot OH \quad (4\text{-}19)$$

$$H_2O_2 + \cdot OH \rightarrow HO_2 \cdot + H_2O \quad (4\text{-}20)$$

$$2HO_2 \cdot \rightarrow H_2O_2 + O_2 \quad (4\text{-}21)$$

$$O_2 +))) \rightarrow 2O \cdot \quad (4\text{-}22)$$

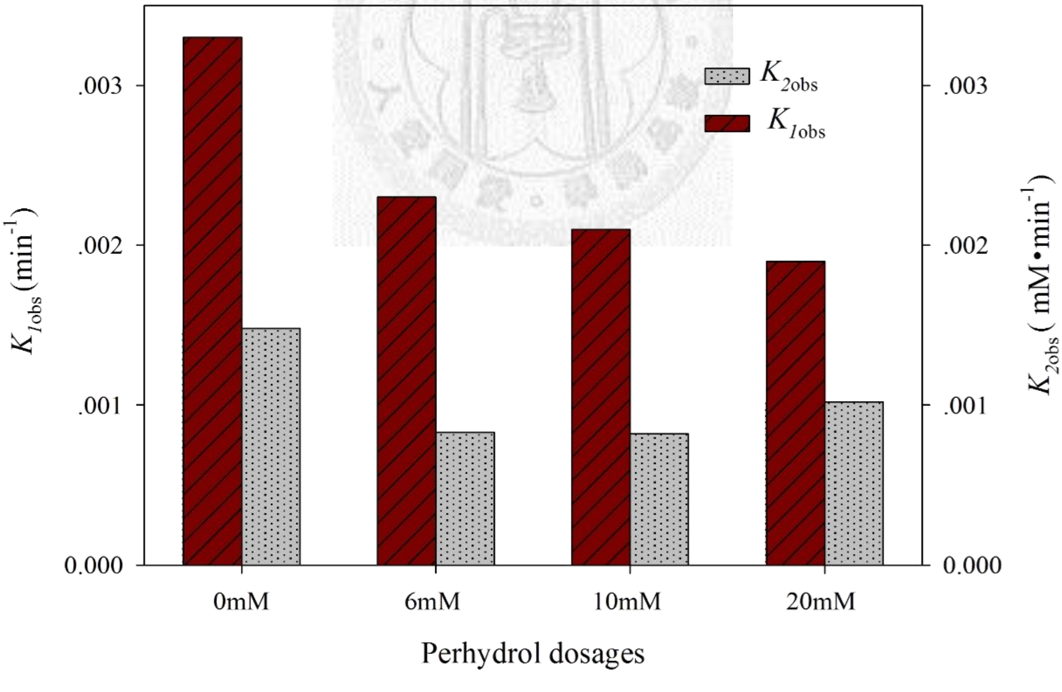

Fig. 4-22 Variation of rate constants of PFOA (132 μM) decomposition (K_{1obs}) and defluorination (K_{2obs}) as a function of H_2O_2 dosages (0, 6, 10, 20 mM) under ultrasonic irradiation (60μm, 150W, 40kHz) with initial solution pH=4 at 30℃.

Therefore, comparison in this section imply that oxygen atmosphere resulting in high dissolved oxygen would suppress the defluorination reaction of PFOA. And argon atmosphere accelerate defluorination process by sweeping away air in the reaction solution.

The effect of perhydrol dosages was carried out in Fig.4-22. It can been seen that raised perhydrol concentration declined rate of PFOA decomposition, while defluorination rate reached its nadir with 6mM perhydrol dosage. More hydroxyl would form more hydroxyl radicals (Eq. (4-19)) under ultrasonic irradiation. However, competitive reaction between hydroxyl radicals and perhydrol (Eq. (4-20)) would produce hydroperoxyl radicals, which were less oxidative than hydroxyl radicals resulting in less activation capacity. Therefore, these opposite effects might lead to the integrated results presented in Fig.4-22.

4.9 Identification of intermediates of PFOA degradation

In PM-US system (60µm, 150W, 40kHz, 10 Mm KMnO4, initial pH=4, without aeration), defluorination efficiency of 74.9% for decomposed PFOA was observed, which is considerably high efficiency and indicates relative little intermediates could be detected. According to the analysis results of IC, PFPrA and TFA are the main intermediates, as portrayed in normalized fluoride mass balance plot (Fig. 4-23), in PM-US system.

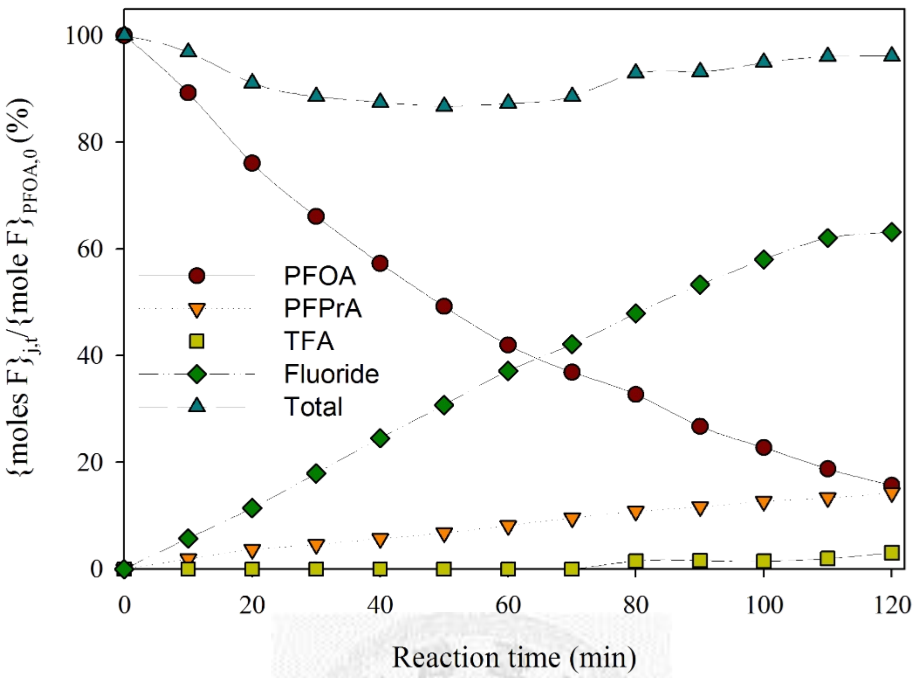

Fig. 4-23 Time dependent analysis of normalized fluorine mass balance during PFOA (132 μM)degradation with 10 mM $KMnO_4$ and initial solution pH=4, under ultrasonic irradiation (60μm, 150W, 40kHz) at 30℃.

Comparative plots of intermediates in different system (PM-US, mono-US and PH-US) were carried out to proof the intermediate species formed under ultrasonic irradiation of this study. As presented in Fig.4-24, same intermediates, PFPrA and TFA, were detected in three degradation systems. PFPrA seemed to form at the beginning of ultrasonication and TFA formed later. The comparison of intermediates concentration also coincide with the degradation rate order: PM-US > mono-US > PH-US. Normalized fluorine mass balance of mono-US and PH-US presented in Fig.4-25 acted as the quality assurance and quality control of intermediates analysis.

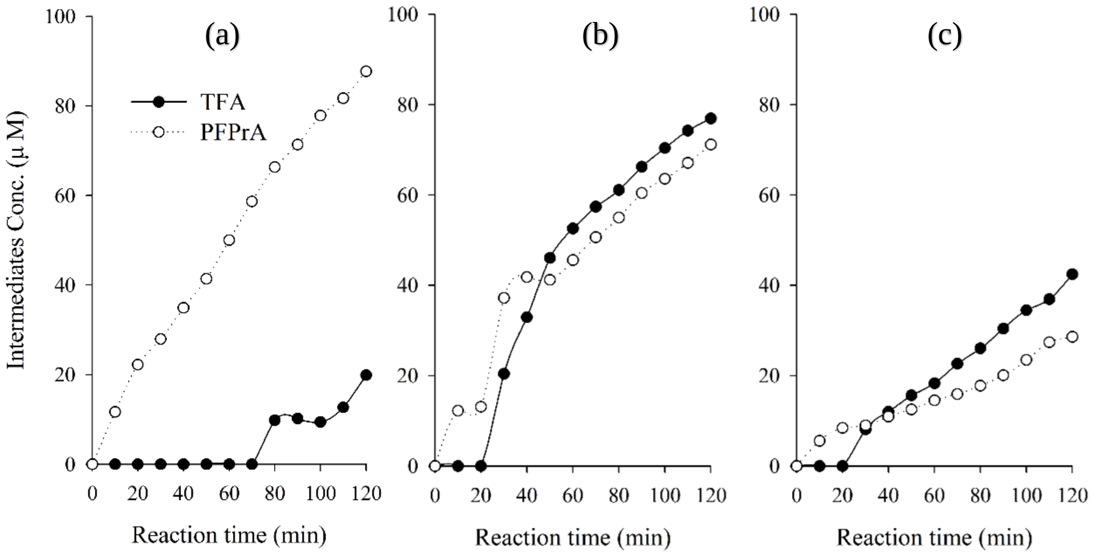

Fig. 4-24 Time dependent variation of intermediates concentration during PFOA (132 μM) degradation in PM-US (a), mono-US (b) and PH-US (c) system, respectively, with 10mM oxidant dosages, initial solution pH=4 and ultrasonic irradiation (60μm, 150W, 40kHz) at 30℃.

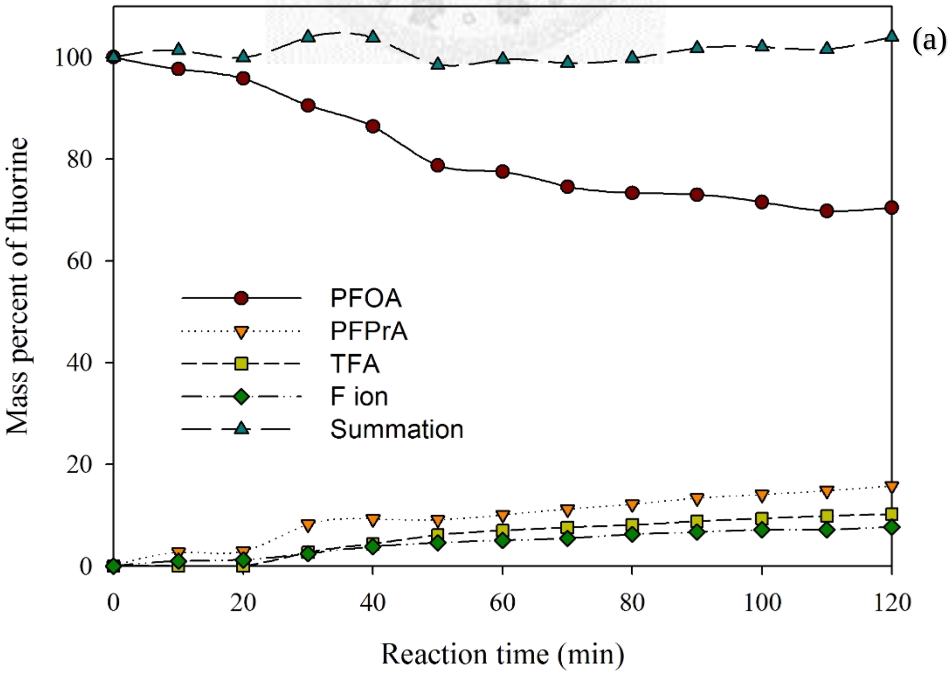

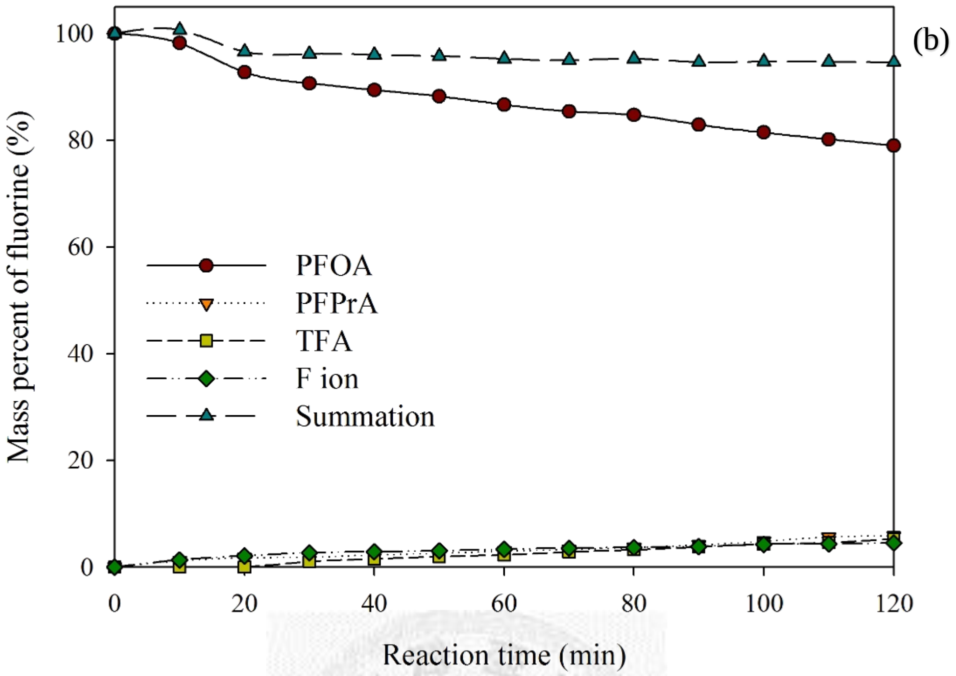

Fig. 4-25 Time dependent analysis of normalized fluorine mass balance during PFOA (132 μM) degradation in mono-US (a) and PH-US (b) system, respectively, with initial solution pH=4 and ultrasonic irradiation (60μm, 150W, 40kHz) at 30℃.

4.10 Proposed mechanisms of PFOA decomposition and defluorination in permanganate-ultrasonic system

The intermediate results are different with that the intermediates $CF_3(CF_2)_nCOO^-$ (n=0-5) were observed in 200W-200kHz system (Moriwaki et al., 2005) and none shorter-chain perfluoro-acid was detected in 150W-618kHz system (Vecitis et al., 2008) .

The discrepancy might be interpreted by the proposed mechanism of PFOA degradation in permanganate-ultrasonic system depicted in Fig. 4-26.

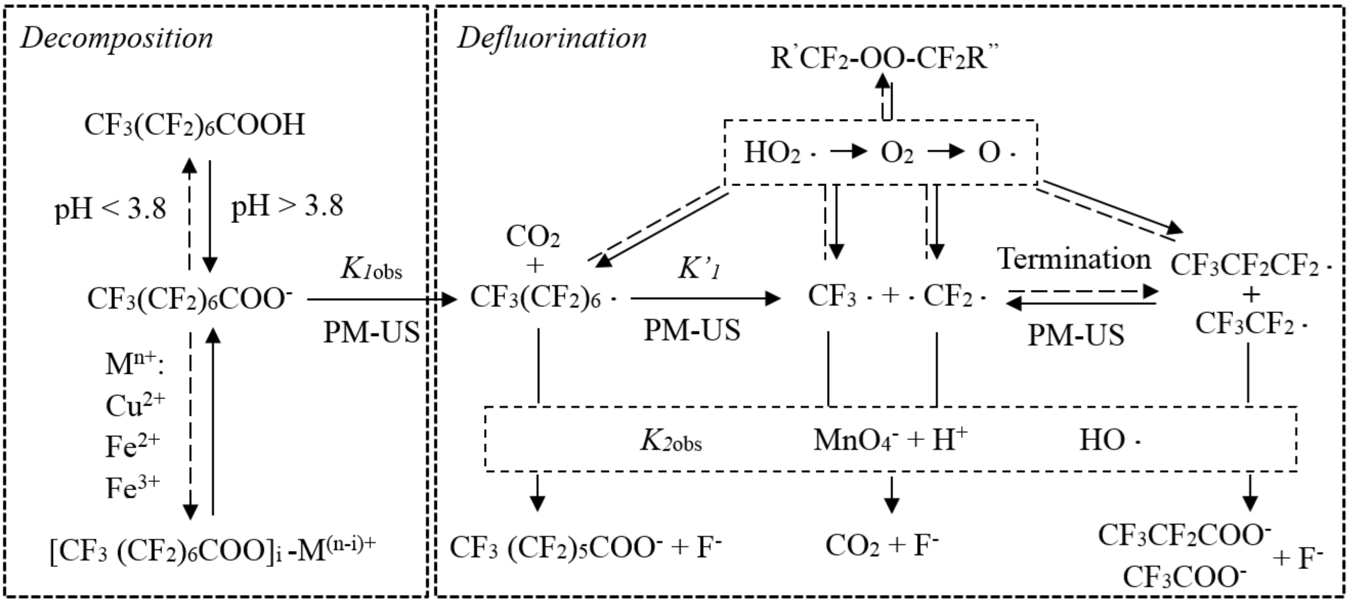

Fig. 4-26 Scheme of proposed mechanism for PFOA degradation, consist of decomposition and defluorination part, in permanganate-ultrasonic system. Solid and dash arrows represent positive reaction and negative effect, respectively, for rate of PFOA decomposition or defluorination.

In PFOA decomposition part, initial cleavage occur in the C-C bond between the perfluorinated tail and the carboxylic group instead of between $-CF_2-$ groups, under permanganate-activated ultrasonic irradiation, due to fluorine stabilize perfluorinated carbon tail via inductively withdrawing electron density on carboxylic group resulting in relatively higher C-C bond energy between $-CF_2-$ groups. Initial cleavage, which step was named PFOA decomposition embodied by rate constant $K_{1\text{obs}}$ throughout this study, yields gaseous carbon dioxide and a perfluoroalkyl radical (Eq. (4-3)). Negative effect, resulting in $K_{1\text{obs}}$ decrease, of highly acidic condition (pH<3.8) and heavy metal cations (M^{n+}) lowered the PFOA concentration on bubble-water interface where synergism between permanganate and ultrasonication works best by transforming PFOA from anions ($CF_3(CF_2)_6COO^-$) to neutral species ($CF_3(CF_2)_6COOH$) and complex form ($[CF_3(CF_2)_6COO]_i$ -$M^{(n-i)+}$) , respectively.

The $CF_3(CF_2)_6\cdot$ radicals, as decomposition products, are initiator of defluorination part and might be oxidized on radical terminal to new carboxylic group ($CF_3(CF_2)_5COO^-$) and fluoride ions. However, as discussed by Vecitis, perfluoroalkyl chemicals in bubble-water interface or internal vapor regions would pyrolyze directly to C_1-fluoro-radical intermediates. Results that high defluorination efficiency and only PFPrA and TFA were detected in this study implied most $CF_3(CF_2)_6\cdot$ radicals continuously decomposed to C_1-perfluoro-radical intermediates ($CF_3\cdot$ and $\cdot CF_2\cdot$), which step, embodied by the rate constant K'_1, is far faster than oxidizing perfluoroalkyl radicals under ultrasonic irradiation for higher energy of C-F bond than C-C bond. It is need to be noticed that $CF_3(CF_2)_6\cdot$ radicals decomposition is a complicated process with different pathway (cleavage of C-C bond in different position) and intermediates (radicals with one to six alkyl units) but similar kinetic rates (Ainagos, 1991) and final products ($CF_3\cdot$ and $\cdot CF_2\cdot$). Therefore, the apparent rate constant K'_1 is crucial for defluorination rate. Coordinating with PFOA decomposition and defluorination rate described in Eq. (4-1) and (4-2), the reaction rate and concentration of $CF_3(CF_2)_6\cdot$ and $C_1\cdot$ (represent $CF_3\cdot$ or $\cdot CF_2\cdot$) radicals can be expressed as follow:

$$\frac{d[CF_3(CF_2)_6\cdot]_i}{dt} = K_{1obs}\cdot[PFOA]_i - K'_1\cdot[CF_3(CF_2)_6\cdot]_i \qquad (4\text{-}23)$$

$$\frac{d[C_1\cdot]_i}{dt} = K'_1\cdot[CF_3(CF_2)_6\cdot]_i - \frac{1}{n}K_{2obs} \qquad (4\text{-}24)$$

$$[CF_3(CF_2)_6\cdot]_i = [PFOA]_0\left[\frac{K_{1obs}}{K'_1 - K_{1obs}}\right][e^{-K_{1obs}t} - e^{-K'_1 t}] \qquad (4\text{-}25)$$

$$[\mathrm{C_1}\cdot]_\mathrm{i} = [\mathrm{PFOA}]_0\left\{1-\frac{1}{K'_1-K_{1\mathrm{obs}}}\left[K'_1\mathrm{e}^{-K_{1\mathrm{obs}}\mathrm{t}}-K_{1\mathrm{obs}}\mathrm{e}^{K'_1\mathrm{t}}\right]\right\}-\frac{1}{\mathrm{n}}K_{2\mathrm{obs}}\mathrm{t} \quad (4\text{-}26)$$

Where n is the average number of fluorine in one $C_1\cdot$ radical.

$C_1\cdot$ radicals would then undergo oxidative defluorination by permanganate and HO· radicals yielding carbon dioxide and fluoride ions which step consist of most PFOA defluorination efficiency. The ionization process (fluoride) can be simulated with pseudo-zero order kinetics imply that abundant of $C_1\cdot$ radicals and oxidants relative to products and oxidation rate. Therefore, some of $CF_3\cdot$ and $\cdot CF_2\cdot$ radicals would remain in solution when stopping ultrasonication or sampling the reaction solution out of ultrasonic system (case in this study). Radicals without ultrasonic irradiation would undergo termination step (see 4.8 section) and form $CF_3CF_2CF_2\cdot$ and $CF_3CF_2\cdot$ radicals as the precursors of detected intermediates PFPrA and TFA, respectively. It can be noticed that TFA were detected after 70 min. This was due to mole ratio of $CF_3\cdot$ to $\cdot CF_2\cdot$ radicals. Clearly, one mole of $CF_3(CF_2)_6\cdot$ radicals would decomposed to one mole $CF_3\cdot$ and six mole $\cdot CF_2\cdot$ radicals. With 1:6 ratio, radicals would form $CF_3CF_2CF_2\cdot$ radicals tendentiously. $\cdot CF_2\cdot$ radicals would oxidize to $\cdot$ CFO with greater rate constant (1.02×10^{-10} $\mathrm{mol\cdot cm^{-3}\cdot s^{-1}}$) than that of oxidation of $CF_3\cdot$ to CF_2O (3.16×10^{-11} $\mathrm{mol\cdot cm^{-3}\cdot s^{-1}}$) (Burgess Jr et al., 1995). Therefore, the mole ratio of $CF_3\cdot$ to $\cdot CF_2\cdot$ would increase and $CF_3CF_2\cdot$ radicals would form as time goes. Formed $CF_3CF_2CF_2\cdot$ and $CF_3CF_2\cdot$ are oxidized to PFPrA and TFA, respectively, with fluoride ions yield as a little part of defluorination efficiency. So PFPrA and TFA can also be called "byproducts".

In view of kinetics order, intermediates discussed above and the bond energies of $F(CF_2)_7$—COO^- (~83 kJ/mol), -CF_2—CF_2- (410 kJ/mol), -C—F (530 kJ/mol), the reaction rates r_1, r'_1 and r_2, simulated with $K_{1\text{obs}}$, K'_1 and $K_{2\text{obs}}$, respectively, could be expected to follow the order: $r_1 > r'_1 > r_2$. In case of ultrasonication last for more than 2 hr, in which PFOA decomposed completely and $C_1\cdot$ radicals were oxidized to a low concentration level that limit defluorination, the kinetics order of defluorination ($K_{2\text{obs}}$) may transition from pseudo-zero-order to first-order.

Oxygen molecule, including hydrogen peroxide, would perform a negative effect on defluorination part via reaction with any perfluoroalkyl radicals. Reaction with oxygen molecules or radicals ($O\cdot$) would finally form perfluoroalkyl esters (Eq. (4-18)) leading to slow down defluorination reaction for needless pathway.

Rate constant of all reaction via “PM-US” way in Fig. 4-26 would be influenced by amplitude of ultrasonic waves, $KMnO_4$ dosages, solution pH and temperature; and ionization process by “$MnO_4^- + H^+$” were directly influenced by $KMnO_4$ dosages, solution pH and temperature.

Table 4-2 Operating parameters of permanganate-ultrasonic system and rate constants of PFOA decomposition and defluorination.

	Operating parameters						Decomposition		Defluorination	
	Dosages [mM]	pH	Amplitude [μm]	Temperature [℃]	Metal [0.2 mM]	Aeration	$K_{1\text{obs}}$ [min^{-1}]	R^2	$K_{2\text{obs}}$ [mM·min^{-1}]	R^2
$KMnO_4$	**0**	4	60	30			0.0033	0.929	0.00148	0.959
	1	4	60	30			0.0044	0.993	0.00261	0.996
	3	4	60	30			0.0127	0.970	0.00570	0.979
	6	4	**60**	**30**			0.0146	0.985	0.00785	0.998
	10	**4**	60	30			0.0153	0.997	0.01088	0.991
	20	4	60	30			0.0159	0.977	0.01201	0.997
	10	**2**	60	30			0.007	0.975	0.00227	0.897
	10	**3**	60	30			0.0143	0.992	0.00576	0.981
	10	**5**	60	30			0.0133	0.994	0.00891	0.992
	10	**7**	60	30			0.0035	0.988	0.00232	0.991
	10	**10**	60	30			0.012	0.987	0.00703	0.996
	10	**11**	60	30			0.0123	0.997	0.01031	0.988
	6	4	**20**	30			0.0021	0.965	0.00168	0.995
	6	4	**40**	30			0.0077	0.977	0.00689	0.987
	6	4	60	**40**			0.016	0.988	0.00807	0.995
	6	4	60	**50**			0.0168	0.994	0.00838	0.997
	6	4	60	30	**Cu(II)**		0.0132	0.975	0.00469	0.988
	6	4	60	30	**Fe(II)**		0.0124	0.987	0.00533	0.989
	6	4	60	30	**Fe(III)**		0.091	0.989	0.00361	0.958
	6	4	60	30		**Argon**	0.0131	0.988	0.01235	0.999
	6	4	60	30		**Oxygen**	0.0099	0.996	0.00563	0.990

Table 4-2 (*Continued*)

	Operating parameters						Decomposition		Defluorination	
	Dosages [mM]	pH	Amplitude [μm]	Temperature [℃]	Metal [0.2 mM]	Aeration	$K_{1\text{obs}}$ [min^{-1}]	R^2	$K_{2\text{obs}}$ [mM·min^{-1}]	R^2
H_2O_2	**6**	4	60	30			0.0023	0.967	0.00083	0.918
	10	4	60	30			0.0021	0.969	0.00082	0.940
	20	4	60	30			0.0019	0.974	0.00102	0.971
	6	4	60	30		**Argon**	0.0026	0.945	0.00199	0.983
	6	4	60	30		**Oxygen**	0.0028	0.963	0.00042	0.932

Chapter 5 Conclusions and prospective

5.1 Conclusions

Permanganate-activated ultrasonic system (PM-US) is a new method to remove PFOA from aqueous solution and ionize fluorine effectively. Amplitude of ultrasonic waves, exemplified to be an influenced operating parameter, would improve $K_{1\mathrm{obs}}$ linearly from 0.0021 min^{-1} to 0.146 min^{-1}. Permanganate dosages, solution pH and temperature influenced the entire process of PFOA degradation, while amplitude directly influenced the PFOA decomposition process. Adverse effect of heavy metal cations was observed on PFOA decomposition via forming complexes with PFOA. Oxygen molecule in reaction solution would lead perfluoroalkyl radicals more likely to undergo termination steps producing more stable radicals and perfluoroalkyl esters resulting in a declined defluorination efficiency. On the contrary, aeration with argon gas increase significantly the defluorination rate. All rate constants of PFOA decomposition and defluorination under various condition in PM-US system were presented and compared in Table 4-2. Exprimental results indicate that PFOA degradation pathways in US-permanganate system comprise: (1) initial cleavage of the C-C bond between the perfluorinated tail and the carboxylic group, yielded carbon dioxide and a perfluoroalkyl radical; (2) continue pyrolysis of perfluoroalkyl radicals on the C-C bonds between -CF_2- units producing $CF_3\cdot$ and $\cdot CF_2\cdot$ radicals (C_1-perfluoro-radicals); (3) oxidation of the generated C_1-perfluoro-radicals producing fluoride ions and gaseous carbon dioxide, which step may be inhibited by oxygen molecule; (4) without ultrasonication, PFPrA and TFA, detected as main degradation intermediates, would form from residual C_1-perfluoro-radicals.

5.2 Prospective

(1) Quantification of perfluoroalkyl radicals

The intermediate steps, stimulated with pseudo-first order kinetics with rate constant K'_1, are significant connection between PFOA decomposition and defluorination. So we can use oxygen gas to induce termination step in ultrasonic system in different irradiation time for stabilizing perfluoroalkyl radicals. In that case, the unstable radical form turn to detectable by LC/MSMS. As a result, the rate constant can be obtained as well to substantialize the kinetics model presented in 4.10.

(2) Effect of bubble size on ultrasonic irradiation and PFOA degradation

Bubbles and its cavitation are main mechanisms for organics degradation in ultrasonic system. So additional bubbles aerated into ultrasonic system might improve the degradation rate. Using aeration rings with various pore sizes to generated different size bubbles can investigate the effect of additional bubbles on sonochemical degradation.

REFERENCES

Ainagos, A., 1991. Mechanism and kinetics of the pyrolysis of normal perfluoroalkanes as illustrated by perfluorohexane. Kinet. Katal 32, 802.

Albano, J., Comfort, S. D., Zlotnik, V., Halihan, T., Burbach, M., Chokejaroenrat, C., Onanong, S. and Clayton, W., 2010. In situ chemical oxidation of rdx-contaminated groundwater with permanganate at the nebraska ordnance plant. Ground Water Monitoring & Remediation 30 (3), 96-106.

Aleboyeh, A., Olya, M. E. and Aleboyeh, H., 2009. Oxidative treatment of azo dyes in aqueous solution by potassium permanganate. Journal of Hazardous Materials 162 (2–3), 1530-1535.

Armitage, J. M., MacLeod, M. and Cousins, I. T., 2009. Modeling the global fate and transport of perfluorooctanoic acid (PFOA) and perfluorooctanoate (PFO) emitted from direct sources using a multispecies mass balance model. Environmental Science & Technology 43 (4), 1134-1140.

Bartlett, P. D. and Traylor, T. G., 1963. Oxygen-18 tracer studies of alkylperoxy radicals. I. The cumylperoxy radical and chain termination in the autoxidation of cumene. Journal of the American Chemical Society 85 (16), 2407-2410.

Beckett, M. A. and Hua, I., 2003. Enhanced sonochemical decomposition of 1,4-dioxane by ferrous iron. Water Research 37 (10), 2372-2376.

Bremner, D. H., Molina, R., Mart ńez, F., Melero, J. A. and Segura, Y., 2009. Degradation of phenolic aqueous solutions by high frequency sono-fenton systems (us–Fe_2O_3/SBA-15–H_2O_2). Applied Catalysis B: Environmental 90 (3–4), 380-388.

Burgess Jr, D. R., Zachariah, M. R., Tsang, W. and Westmoreland, P. R., 1995.

Thermochemical and chemical kinetic data for fluorinated hydrocarbons. Progress in Energy and Combustion Science 21 (6), 453-529.

Burns, D. C., Ellis, D. A., Li, H., McMurdo, C. J. and Webster, E., 2008. Experimental pK_a determination for perfluorooctanoic acid (PFOA) and the potential impact of pK_a concentration dependence on laboratory-measured partitioning phenomena and environmental modeling. Environmental Science & Technology 42 (24), 9283-9288.

Cao, M. H., Wang, B. B., Yu, H. S., Wang, L. L., Yuan, S. H. and Chen, J., 2010. Photochemical decomposition of perfluorooctanoic acid in aqueous periodate with VUV and UV light irradiation. Journal of Hazardous Materials 179 (1–3), 1143-1146.

Cheng, J., Vecitis, C. D., Park, H., Mader, B. T. and Hoffmann, M. R., 2008. Sonochemical degradation of perfluorooctane sulfonate (PFOS) and perfluorooctanoate (PFOA) in landfill groundwater: Environmental matrix effects. Environmental Science & Technology 42 (21), 8057-8063.

Cheng, J., Vecitis, C. D., Park, H., Mader, B. T. and Hoffmann, M. R., 2009. Sonochemical degradation of perfluorooctane sulfonate (PFOS) and perfluorooctanoate (PFOA) in groundwater: Kinetic effects of matrix inorganics. Environmental Science & Technology 44 (1), 445-450.

Colosi, L. M., Pinto, R. A., Huang, Q. and Weber, W. J., Jr., 2009. Peroxidase-mediated degradation of perfluorooctanoic acid. Environmental Toxicology and Chemistry 28 (2), 264-271.

Croiset, E., Rice, S. F. and Hanush, R. G., 1997. Hydrogen peroxide decomposition in supercritical water. AIChE Journal 43 (9), 2343-2352.

Damm, J. H., Hardacre, C., Kalin, R. M. and Walsh, K. P., 2002. Kinetics of the oxidation of methyl tert-butyl ether (MTBE) by potassium permanganate. Water Research 36 (14), 3638-3646.

Giri, R. R., Ozaki, H., Okada, T., Taniguchi, S. and Takanami, R., 2012. Factors influencing UV photodecomposition of perfluorooctanoic acid in water. Chemical Engineering Journal 180 (0), 197-203.

Goskonda, S., James Catallo, W. and Junk, T., 2002. Sonochemical degradation of aromatic organic pollutants. Waste Management 22 (3), 351-356.

Han, Q., Dong, W., Wang, H., Liu, T., Sun, F., Ying, Y. and Yan, X., 2013. Effects of coexisting anions on decolorization of azo dye X-3B by ferrate(VI) and a comparative study between ferrate(VI) and potassium permanganate. Separation and Purification Technology 108 (0), 74-82.

Hori, H., Hayakawa, E., Einaga, H., Kutsuna, S., Koike, K., Ibusuki, T., Kiatagawa, H. and Arakawa, R., 2004. Decomposition of environmentally persistent perfluorooctanoic acid in water by photochemical approaches. Environmental Science & Technology 38 (22), 6118-6124.

Hori, H., Yamamoto, A., Hayakawa, E., Taniyasu, S., Yamashita, N., Kutsuna, S., Kiatagawa, H. and Arakawa, R., 2005. Efficient decomposition of environmentally persistent perfluorocarboxylic acids by use of persulfate as a photochemical oxidant. Environmental Science & Technology 39 (7), 2383-2388.

Hori, H., Yamamoto, A., Koike, K., Kutsuna, S., Osaka, I. and Arakawa, R., 2007. Photochemical decomposition of environmentally persistent short-chain perfluorocarboxylic acids in water mediated by iron(II)/(III) redox reactions. Chemosphere 68 (3), 572-578.

Houde, M., Martin, J. W., Letcher, R. J., Solomon, K. R. and Muir, D. C. G., 2006. Biological monitoring of polyfluoroalkyl substances: A review. Environmental Science & Technology 40 (11), 3463-3473.

Jiang, Y., Petrier, C. and Waite, T. D., 2006. Sonolysis of 4-chlorophenol in aqueous solution: Effects of substrate concentration, aqueous temperature and ultrasonic frequency. Ultrasonics Sonochemistry 13 (5), 415-422.

Joseph, J. M., Destaillats, H., Hung, H.-M. and Hoffmann, M. R., 1999. The sonochemical degradation of azobenzene and related azo dyes: Rate enhancements via fenton's reactions. The Journal of Physical Chemistry A 104 (2), 301-307.

Kaiser, M. A., Larsen, B. S., Kao, C.-P. C. and Buck, R. C., 2005. Vapor pressures of perfluorooctanoic, -nonanoic, -decanoic, -undecanoic, and -dodecanoic acids. Journal of Chemical & Engineering Data 50 (6), 1841-1843.

Key, B. D., Howell, R. D. and Criddle, C. S., 1997. Fluorinated organics in the biosphere. Environmental Science & Technology 31 (9), 2445-2454.

Kutsuna, S. and Hori, H., 2008. Experimental determination of henry's law constant of perfluorooctanoic acid (PFOA) at 298 k by means of an inert-gas stripping method with a helical plate. Atmospheric Environment 42 (39), 8883-8892.

Lau, C., Anitole, K., Hodes, C., Lai, D., Pfahles-Hutchens, A. and Seed, J., 2007. Perfluoroalkyl acids: A review of monitoring and toxicological findings. Toxicological Sciences 99 (2), 366-394.

Lee, Y.-C., Lo, S.-L., Chiueh, P.-T. and Chang, D.-G., 2009. Efficient decomposition of perfluorocarboxylic acids in aqueous solution using microwave-induced persulfate. Water Research 43 (11), 2811-2816.

Lee, Y.-C., Lo, S.-L., Chiueh, P.-T., Liou, Y.-H. and Chen, M.-L., 2010. Microwave-hydrothermal decomposition of perfluorooctanoic acid in water by iron-activated persulfate oxidation. Water Research 44 (3), 886-892.

Liu, C., Qiang, Z., Adams, C., Tian, F. and Zhang, T., 2009. Kinetics and mechanism for degradation of dichlorvos by permanganate in drinking water treatment. Water Research 43 (14), 3435-3442.

Loos, R., Locoro, G., Comero, S., Contini, S., Schwesig, D., Werres, F., Balsaa, P., Gans, O., Weiss, S. and Blaha, L., 2010. Pan-european survey on the occurrence of selected polar organic persistent pollutants in ground water. Water Research 44 (14), 4115-4126.

Malhotra, S. L., 1986. Ultrasonic solution degradations of poly(alkyl methacrylates). Journal of Macromolecular Science: Part A - Chemistry 23 (6), 729-748.

Melzer, D., Rice, N., Depledge, M. H., Henley, W. E. and Galloway, T. S., 2010. Association between serum perfluorooctanoic acid (PFOA) and thyroid disease in the us national health and nutrition examination survey. Environmental health perspectives 118 (5), 686.

Morel, F. M. M. and Hering, J. G. (1993). Principles and applications of aquatic chemistry, John Wiley & Sons.

Moriwaki, H., Takagi, Y., Tanaka, M., Tsuruho, K., Okitsu, K. and Maeda, Y., 2005. Sonochemical decomposition of perfluorooctane sulfonate and perfluorooctanoic acid. Environmental Science & Technology 39 (9), 3388-3392.

Nagata, Y., Hirai, K., Bandow, H. and Maeda, Y., 1996. Decomposition of hydroxybenzoic and humic acids in water by ultrasonic irradiation. Environmental Science & Technology 30 (4), 1133-1138.

Ochiai, T., Iizuka, Y., Nakata, K., Murakami, T., Tryk, D. A., Fujishima, A., Koide, Y. and Morito, Y., 2011. Efficient electrochemical decomposition of perfluorocarboxylic acids by the use of a boron-doped diamond electrode. Diamond and Related Materials 20 (2), 64-67.

Ochoa-Herrera, V. and Sierra-Alvarez, R., 2008. Removal of perfluorinated surfactants by sorption onto granular activated carbon, zeolite and sludge. Chemosphere 72 (10), 1588-1593.

Olya, M., Aleboyeh, H. and Aleboyeh, A., 2012. Decomposition of a diazo dye in aqueous solutions by $KMnO_4/UV/H_2O_2$ process Progress in Color, Colorants and Coatings 5, 41-46.

Post, G. B., Cohn, P. D. and Cooper, K. R., 2012. Perfluorooctanoic acid (PFOA), an emerging drinking water contaminant: A critical review of recent literature. Environmental Research 116 (0), 93-117.

Prevedouros, K., Cousins, I. T., Buck, R. C. and Korzeniowski, S. H., 2005. Sources, fate and transport of perfluorocarboxylates. Environmental Science & Technology 40 (1), 32-44.

Price, G. J. and Smith, P. F., 1993. Ultrasonic degradation of polymer solutions: 2. The effect of temperature, ultrasound intensity and dissolved gases on polystyrene in toluene. Polymer 34 (19), 4111-4117.

Qu, Y., Zhang, C., Li, F., Chen, J. and Zhou, Q., 2010. Photo-reductive defluorination of perfluorooctanoic acid in water. Water Research 44 (9), 2939-2947.

Rajenden, R. (2000). Aeration, water treatment. Kirk-othmer encyclopedia of chemical technology, John Wiley & Sons, Inc.

Raso, J., Mañas, P., Pagán, R. and Sala, F. J., 1999. Influence of different factors on the output power transferred into medium by ultrasound. Ultrasonics Sonochemistry 5 (4), 157-162.

Sakurai, T., Nagazumi, H., Hijii, K., Suzuta, T., Kudo, M., Yoshino, K., Kubota, T., Kubota, T., Kagawa, H. and Ikeda, Y.,1998. Ultrasonic treatment apparatus, Google

Patents.

Siegrist, R. L., Urynowicz, M. A., West, O. R., Crimi, M. L. and Lowe, K. S. (2001). Principles and practices of in situ chemical oxidation using permanganate, Battelle Press Columbus, OH.

Sri Chandana Panchangam, Lin, A. Y.-C., Tsai, J.-H., Lin, C.-F., 2009. Sonication-assisted photocatalytic decomposition of perfluorooctanoic acid. Chemosphere 75, 654-660.

Suslick, K. S., 1990. Acoustic cavitation in homogeneous liquids. Science (New York, N.Y.) 247, 1439-1445.

Suslick, K. S., Gawienowski, J. J., Schubert, P. F. and Wang, H. H., 1983. Alkane sonochemistry. The Journal of Physical Chemistry 87 (13), 2299-2301.

Tang, H., Xiang, Q., Lei, M., Yan, J., Zhu, L. and Zou, J., 2012. Efficient degradation of perfluorooctanoic acid by UV–fenton process. Chemical Engineering Journal 184 (0), 156-162.

Vecitis, C. D., Park, H., Cheng, J., Mader, B. T. and Hoffmann, M. R., 2008. Kinetics and mechanism of the sonolytic conversion of the aqueous perfluorinated surfactants, perfluorooctanoate (PFOA), and perfluorooctane sulfonate (PFOS) into inorganic products. The Journal of Physical Chemistry A 112 (18), 4261-4270.

Vestergren, R. and Cousins, I. T., 2009. Tracking the pathways of human exposure to perfluorocarboxylates. Environmental Science & Technology 43 (15), 5565-5575.

Walton, J., Labine, P. and Reidies, A., 1991. The chemistry of permanganate in degradative oxidations. Chemical Oxidation, Technomic Publishing Co. Inc., Lancaster, Basel, 205-219.

Wang, Y., Zhang, P., Pan, G. and Chen, H., 2008. Ferric ion mediated photochemical decomposition of perfluorooctanoic acid (PFOA) by 254nm UV light. Journal of Hazardous Materials 160 (1), 181-186.

Wu, Z. L., Lifka, J. and Ondruschka, B., 2006. Comparison of energy efficiency of various ultrasonic devices in aquasonochemical reactions. Chemical Engineering & Technology 29 (5), 610-615.

Yan, Y. E. and Schwartz, F. W., 1999. Oxidative degradation and kinetics of chlorinated ethylenes by potassium permanganate. Journal of Contaminant Hydrology 37 (3–4), 343-365.

Yim, B., Okuno, H., Nagata, Y., Nishimura, R. and Maeda, Y., 2002. Sonolysis of surfactants in aqueous solutions: An accumulation of solute in the interfacial region of the cavitation bubbles. Ultrasonics Sonochemistry 9 (4), 209-213.

Zareitalabad, P., Siemens, J., Hamer, M. and Amelung, W., 2013. Perfluorooctanoic acid (PFOA) and perfluorooctanesulfonic acid (PFOS) in surface waters, sediments, soils and wastewater – a review on concentrations and distribution coefficients. Chemosphere 91 (6), 725-732.

Zhao, B. and Zhang, P., 2009. Photocatalytic decomposition of perfluorooctanoic acid with β-Ga_2O_3 wide bandgap photocatalyst. Catalysis Communications 10 (8), 1184-1187.

Zhao, H., Gao, J., Zhao, G., Fan, J., Wang, Y. and Wang, Y., 2013. Fabrication of novel SnO_2-Sb/carbon aerogel electrode for ultrasonic electrochemical oxidation of perfluorooctanoate with high catalytic efficiency. Applied Catalysis B: Environmental 136–137 (0), 278-286.